

Frequency Sharing for Radio Local Area Networks in the 6 GHz Band (Version 2.0)

August 2021

Prepared by:

RKF Engineering Solutions, LLC
7500 Old Georgetown Road
Bethesda, MD



Prepared for:

Instituto Federal de Telecomunicaciones - Mexico

1 Table of Contents

1	Table of Contents	2
1.0	Executive Summary	4
1.1	Fixed Satellite Service (FSS)	5
1.2	Fixed Service (FS)	5
1.3	Mobile Satellite Service (MSS) Gateway	6
2	Introduction	7
2.1	Background on Three Classes of RLANs	8
2.2	Approach	9
3	RLAN Deployment and Operating Assumptions	10
3.1	RLAN Deployment Assumptions	10
3.1.1	Number of Active RLANs and Deployment Distribution	10
3.1.2	Population Density	14
3.2	RLAN Operating Assumptions	14
3.2.1	Distribution of Source LPI and Standard Power RLAN Power Levels	15
3.2.2	Body Loss for LPI and Standard Power Indoor and Outdoor devices	21
3.2.3	Distribution of Source VLP Power Levels including Body Loss	21
3.2.4	Bandwidth and Channel Distribution	22
3.2.3	Distribution of RLAN heights	22
4	Propagation Models	24
4.1	RLAN to FSS Propagation Models (Earth to Space)	24
4.2	RLAN to Terrestrial FS Propagation Models	25
4.3	RLAN to Terrestrial MSS Gateway Models	27
5	Sharing Results	27
5.1	FSS Uplink Sharing	27
5.1.1	FSS Simulation Methodology	28
5.1.2	RLAN Populations used in the Simulations	31
5.1.3	Results by FSS Satellite Beam	32
5.1.3.1	Satmex 8 (116.8° W)	32
5.1.3.2	Eutelsat 115 West-B (Satmex 7) (114.9° W)	33
5.1.3.3	Satmex 6 (113° W)	34
5.1.3.4	SES-3 (103° W)	36
5.1.3.5	Galaxy-19 (97° W)	37
5.1.3.6	NSS-806 (47.5° W)	38
5.1.4	FSS Link Budgets	39

5.1.5	FSS Sharing Conclusions	40
5.2	Fixed Service (FS) Sharing	40
5.2.1	FS Database	40
5.2.2	Key Modeling Assumptions	44
5.2.2.1	RLAN Device Deployment	44
5.2.2.2	FS Receiver Antenna Performance	44
5.2.2.3	FS Simulation Methodology	45
5.2.3	Aggregate Interference Simulation	46
5.2.4	FS Availability Analysis	48
5.2.5	FS Sharing Conclusions	53
5.3	MSS Gateway Coexistence	53
5.3.1	MSS Gateway Characteristics	54
5.3.2	RLAN Device Characteristics	56
5.3.3	MSS Simulation Methodology	57
5.3.4	MSS Simulation Results	59
5.3.5	MSS Gateway Coexistence Sharing Conclusion	60

1.0 Executive Summary

This study responds to the Consultation issued by the Institute Federal de Telecomunicaciones (IFT) regarding the prospective use of the 5.925 to 7.125 GHz band (“6 GHz band”).¹ The IFT raises questions about the potential use of the band by license-exempt devices, such as Radio Local Area Networks (RLANs).² The Consultation asks questions about three different types of RLANs (collectively referred to as RLANs in this report):

- Low Power Indoor (LPI)
- Standard Power (indoor/outdoor) with Automated Frequency Coordination (AFC)
- Very Low Power (VLP) (indoor/outdoor)

The Consultation also asks questions regarding whether such RLAN use is compatible with existing incumbent services in the band.

To assist in answering these questions, RKF Engineering Solutions, LLC (RKF), analyzed the potential impact of license-exempt RLANs on three types of incumbent users in the band: Fixed Satellite Service (FSS), Fixed Service (FS), and Mobile Satellite Service (MSS). In Mexico, the 6 GHz band is shared primarily by two services: FSS uplinks³ and fixed microwave (Fixed Service or FS) links. Additionally, there had been a single MSS feeder downlink site in Mexico that was taken off-line a few years ago. Construction is underway to establish a new MSS feeder downlink “gateway” site at a new location outside of Mexico City.

As IFT recognizes in its Reference Document,⁴ the three identified classes of RLANs are based on rules that have been proposed by other regulatory authorities, including the US Federal Communications Commission, Ofcom in the United Kingdom and by the Electronic Communications Committee (ECC) of the European Conference of Postal and Telecommunications Administrations (CEPT). The technical specifications of these device classes are intended to allow for coexistence between RLANs and incumbent users of the band, including Fixed Service links (FS), fixed satellite uplink (FSS), and the Mobile Satellite Service MSS feeder downlink.

This study examines the coexistence of RLAN usage in the 6 GHz band and incumbent FSS satellite uplink services in Mexico. In addition, this study examines the impact of RLAN usage for a subset of FS links in Mexico City. This study assumes a number of instantaneously transmitting RLAN devices in Monte-Carlo simulations to understand the interference risk to FSS and FS operations in Mexico. Finally, the study examines the interference risk to the MSS feeder downlink from each class (and total number) of RLAN devices operating within 150 km from the new MSS gateway site.

¹ Public Consultation of Integration of the “Frequency Band Questionnaire 5925-7125 MHz,” Institute Federal de Telecomunicaciones (5 November 2020) <http://www.ift.org.mx/industria/consultas-publicas/consulta-publica-de-integracion-del-cuestionario-sobre-la-banda-de-frecuencias-5925-7125-mhz> (“Consultation”).

² RLAN is a generic term used to describe a device that provides local area network connections between various electronic devices. While Wi-Fi is one type of RLAN, this study applies to other RLANs with Unlicensed National Information Infrastructure (U-NII) operating characteristics.

³ Paired with FSS downlinks in 3.4-4.2 GHz band.

⁴ IFT Reference Document, Frequency Band 5925-7125 MHz, October 2020 available at <http://www.ift.org.mx/industria/consultas-publicas/consulta-publica-de-integracion-del-cuestionario-sobre-la-banda-de-frecuencias-5925-7125-mhz> (“IFT Reference Document”).

This study used data based on the population density in Mexico, as well as projected consumer and business RLAN usage patterns in terms of the time of use and the location (indoor/outdoor). In addition, the study accounted for the impact of body loss, indoor use, and the bandwidth and channel distribution of the RLAN devices on coexistence.

The analysis showed that RLAN operation in Mexico in the entire 6 GHz band will not cause harmful interference to FSS or FS incumbents, as well as the earth station antenna at the MSS gateway site.

1.1 Fixed Satellite Service (FSS)

In the 6 GHz uplink band, the aggregate I/N into a number of satellite uplink beams was computed using Monte-Carlo simulations with random RLAN deployments and available satellite G/T contours. The RLANs were deployed in Mexico as well as all other countries within each satellite's view. For a conservative analysis, satellite beams with higher G/T over Mexico or bigger coverage of areas had been chosen. Information on the FSS filings was extracted from the International Telecommunication Union (ITU) Radiocommunication Bureau (BR) International Frequency Information Circular (IFIC) Space Services database.

The analysis has been applied to a satellite channel plan assuming 36 MHz channels in 40 MHz occupied bandwidth on two polarizations. Each channel on each satellite has been subject to 10 independent RLAN deployments of a Monte Carlo simulation.

Simulations show that in all cases studied, the I/N for all satellites in all channels and simulation iterations is less than -26.92 dB. It can be concluded that a deployment of RLANs in the field of view of the affected satellites will not impact the operation of the Mexican FSS uplinks in the 6 GHz band.

In conclusion, RLANs in the three device classes operating over a 20, 40, 80, or 160 MHz channel bandwidth do not cause harmful interference to an FSS uplink.

1.2 Fixed Service (FS)

Monte-Carlo simulations were performed with random RLAN deployments to understand the interference risk to FS operations in Mexico. The simulation consisted of 100,000 RLAN deployment iterations to gather stable, long-term interference statistics at each of 27 FS sites around Mexico City.

Statistics were gathered at each FS, on the occurrence probabilities for both $I/N > -6$ dB and 0 dB. Because these metrics do not fully describe the interference risk, an additional metric, increased FS unavailability due to RLAN interference, was used to assess degradation in FS performance. This analysis assumed a typical FS design target of 99.999% availability (unavailability=0.001% corresponding to 5.3 minutes/year). Results were compared to a target increase in unavailability of less than 10% (availability with interference $>99.9989\%$) sufficient to allow continued robustness of FS links while also allowing the new RLAN service. Sensitivity to a 1% increase in unavailability was also considered.

The I/N > -6 dB and 0 dB average occurrence probability of a single FS was 0.209% and 0.035% respectively for the Baseline Simulations.

For the FS availability analysis, the increase in unavailability due to RLAN interference of the 27 FS links was further analyzed in two steps. In the first step, a representative link margin required to meet the target availability was calculated without considering the specific operational parameters of each FS link. This simplified analysis allowed a large number of links to be processed. In the second step, if the simplified analysis indicated an FS link did not meet the target 10% unavailability increase, individual FS operational parameters were analyzed to determine the actual increase in unavailability. This analysis provided a realistic assessment of the long-term impact of the RLAN interference on FS stations and showed **all 27 links met the 10% increase in unavailability target as well as the 1% increase in unavailability sensitivity threshold.**

In conclusion, our analysis showed that RLAN operation within the parameters of the three device classes described in this report, at a variety of channel sizes, will not cause harmful interference to FS stations. In addition, sensitivity analyses on parameters including bandwidth, number of active devices, and EIRP indicated that in all cases the probability of an I/N > -6 dB occurrence was low and the increase in unavailability was sufficiently low to allow continued robustness of FS links.

1.3 Mobile Satellite Service (MSS) Gateway

A Monte-Carlo Simulation was performed using 100,000 iterations of randomly deployed RLANs to calculate the aggregate signal received by the MSS earth station antenna from each class of RLANs within 150 km of the new MSS gateway location.

The geo-coordinates and operating characteristics of the MSS downlink receiving earth station, located in an isolated valley west of Mexico City, were taken from the MSS gateway operator's license application. At the new MSS gateway site under construction, a single earth station antenna was selected. The MSS constellation's movement as viewed from the MSS receiving station was simulated over time. For a randomly selected moment, one of the satellites in view above the radio horizon was chosen. There were 20,000 iterations of the MSS constellation's movement. In each simulation iteration, the pointing direction of the earth station antenna was chosen randomly. A cumulative distribution function (CDF) of the earth station antenna elevation angle was generated.

The simulation examined the effect on the (victim) earth station antenna of the randomly selected pointing angles and RLAN placements over the large number of iterations. The simulation generated separate CDFs for LPI, Standard Power, VLP, and total RLAN devices for I/N > -6 dB and I/N > -12.2 dB. The results show that the cumulative probabilities of an I/N > -6 and I/N > -12.2 are very low for all three RLAN classes and well within the expected range for total RLANs. The CDF for an I/N > -6 are 0.031%, 0.049%, and 0.003% respectively for Standard Power, LPI and VLP devices. For an I/N > -12.2, the CDF values increase to 0.070%, 0.146% and 0.006% respectively for Standard Power, LPI, and VLP devices. The conclusion is that the risk of harmful interference to the MSS earth station receiver is extremely low.

2 Introduction

Devices that employ Wi-Fi and other unlicensed standards have become indispensable for providing low-cost wireless connectivity in countless products used by Mexican consumers. License-exempt technologies are a critical element in delivering broadband connectivity to consumers and businesses. Wi-Fi is needed to connect all devices in a household or business to a wired or wireless broadband connection. As consumers rely on more devices, reliable and fast Wi-Fi connectivity has become essential. However, despite the increasing reliance on license-exempt technology, and the enormous growth in traffic demands being placed on the technology globally, the spectrum allocated to Wi-Fi use remains limited to the 2.4 GHz and 5 GHz bands as it has for many years.

The latest Wi-Fi technology—designed for speed, low latency and to optimize use by many devices in the same location—uses much wider channelization to meet the far more intensive broadband needs of consumers and businesses alike. For example, the latest generation of Wi-Fi technology, Wi-Fi 6, can utilize radio channels as broad as 80 or 160 megahertz, and a future generation of Wi-Fi technology that is already in development will utilize channels of 320 megahertz.⁵

For these reasons, on April 23, 2020, the Federal Communications Committee in the United States (the FCC) adopted rules⁶ that made 1200 MHz of spectrum available in the 6 GHz band (5.925-7.125 GHz) for license-exempt use. These new rules will expand license-exempt broadband operations that promise to bring a wide range of innovative wireless applications to consumers while protecting incumbent users in the band. As has occurred with Wi-Fi in the 2.4 GHz and 5 GHz bands, it is expected that the rules adopted for 6 GHz unlicensed devices will foster the expansion of Wi-Fi hotspot networks to provide consumers access to even higher speed data connections and growth in the Internet-of-things (IoT) industry—connecting appliances, machines, meters, wearables, and other consumer electronics, as well as industrial sensors for manufacturing. This capability will quickly become a part of peoples’ everyday lives.

In this study, produced in response to the IFT’s consultation on the 6 GHz band, RKF used a proven methodology to model a Monte Carlo simulation of coexistence. This methodology was used in the studies submitted before the US FCC.

The study is focused on examining coexistence between the three classes of RLANs (Standard-Power AFC, LPI, and VLP) and the uplink of Mexico’s FSS satellites in the 5925-6425 MHz band. To produce results for Mexico, RKF used data based on the population distribution and

⁵“Wi-Fi 6 Certified, Capacity, efficiency, and performance for advanced connectivity,” Wi-Fi Alliance, <https://www.wi-fi.org/discover-wi-fi/wi-fi-certified-6>. There are a number of technological improvements contained in Wi-Fi 6 that make this generation of technology the most spectrally efficient version of Wi-Fi in history, including multi-user MIMO, beamforming, and “target wake time” to improve network efficiency and device battery life. When deployed in 6 GHz, Wi-Fi 6 will be called Wi-Fi 6E.

⁶ See *Unlicensed Use of the 6 GHz Band*, Report and Order and Further Notice of Proposed Rulemaking, ET Docket No. 18-295, FCC 20-51 (rel. Apr. 23, 2020) at https://ecfsapi.fcc.gov/file/0424167164769/FCC-20-51A1_Rcd.pdf. (“6 GHz Report and Order”).

density in Mexico, as well as projected consumer and business RLAN usage patterns in terms of the time of use and the location (indoor/outdoor). In addition, the study accounted for the impact of body loss, indoor use, and the bandwidth and channel distribution of the RLAN devices on coexistence.

RKF obtained Mexico FSS uplink data from BR International Frequency Information Circular (Space Services) (BR IFIC).

The data for FS links in the vicinity of Mexico City and the MSS gateway were provided by the IFT.

2.1 Background on Three Classes of RLANs

This analysis included the three classes of RLANs recognized by the IFT in its Reference Document.⁷ This device class framework that has been established by the FCC⁸ as well as the United Kingdom⁹ and Europe.¹⁰

Low Power Indoor: The FCC authorized LPI access points and client devices across the entire 6 GHz band and do not rely on the AFC system for determining the frequencies available for use. These low-power access points will be ideal for connecting devices in homes and businesses, such as smartphones, tablet devices, laptops, and IoT devices, to the Internet. Using these advanced Wi-Fi technologies and wider channels (up to 320 MHz) available in the 6 GHz band, unlicensed devices promise to spur innovations and allow consumers to experience faster internet connections and new applications well beyond what is possible with 2.4 GHz and 5 GHz bands.

Very Low Power portable: The FCC has an active rulemaking proceeding considering VLP portable (indoor/outdoor) devices in the 6 GHz band at 14 dBm EIRP. The United Kingdom adopted this class of RLANs, and Europe is poised to adopt the same.¹¹ Portable VLP devices will expand innovation even further and will be critical for supporting indoor and outdoor portable use cases such as wearable peripherals including augmented reality/virtual reality as well as in-vehicle applications and other personal-area-network applications.

Standard Power with AFC: The FCC authorized Standard Power with AFC access points but restricted them to operate within the UN-II 5 (5925-6425 MHz) and UN-II 7 (6525-6875 MHz) portions of the band. The AFC system determines the frequencies on which Standard Power access points operate without causing harmful interference to incumbent microwave receivers and then identifies those frequencies as available for use by Standard Power access points.

⁷ IFT Reference Document at 18-31.

⁸ See 6 GHz Report and Order (adopting low power indoor and standard power with AFC and proposing VLP in its Further Notice of Proposed Rulemaking).

⁹ The UK adopted LPI and VLP in the lower 500 MHz of the 6 GHz band. Statement:Improving Spectrum access for wifi—spectrum use in the 5 and 6 GHz bands (24 July 2020) available at https://www.ofcom.org.uk/_data/assets/pdf_file/0036/198927/6ghz-statement.pdf

¹⁰ The Electronic Communication Committee approved the [ECC Decision 20\(01\)](#) and the [CEPT Report 75](#) during its plenary meeting 16-20th November 2020. This Decision supports LPI and VLP in the lower 500 MHz of the 6 GHz band.

¹¹ Cite

2.2 Approach

A detailed nationwide simulation of the interference environment was developed and RKF ensured its simulation was a conservative representation of the interference environment by:

- 1) Analyzing FSS beams susceptible to highest interference levels. The BR International Frequency Information Circular (Space Services) (BR IFIC) was used to extract the FSS filings;
- 2) Using the Gridded Population of the World V4 (GPWv4) from NASA's Socioeconomic Data and Applications Center (SEDAC). GPWv4 provides a global composite raster grid of population density at 30 arcsecond resolution (approximately 1 km at the equator) using population estimates for the years 2000, 2005, 2010, 2015 and 2020. This dataset can also be supplemented with national population projections from other sources for intermediate or extrapolated years through linear scaling approximations over administration boundaries. The population of Mexico, as well as the Americas and other areas in the view of the simulated Satellites, in 2025 has been calculated on the basis of the 2018 edition of the UN World Population Prospects;
- 3) Using realistic but conservative RLAN operating and deployment assumptions as described in Section 3.0. These were based on existing and projected market data, usage, and performance;
- 4) Using worst case scenarios to represent possible situations;
- 5) Executing numerous different scenarios with a wide variation of propagation paths and RLAN deployment configurations to ensure statistically significant results. US Census Bureau (USCB) definitions are used to partition the Mexico into urban, suburban, and rural areas and the GWPv4 2025 projected Mexico population density was used to randomly deploy RLANs for each simulation iteration;
- 6) An I/N of -6 dB was used as a comparison threshold for the FS in this study with the understanding that the analysis in this report is very conservative and did not take into account many factors that would lower the aggregate I/N.
- 7) The MSS gateway study used I/N values of -6 dB and -12.2 dB as comparison thresholds. Similar to the FS study, the analysis is conservative and did not take into account factors that would lower the aggregate I/N.

Simulation results and sharing studies with FSS uplinks are covered in Section 5.1, FS links in Section 5.2, and the MSS gateway in Section 5.3.

3 RLAN Deployment and Operating Assumptions

This section describes the analysis and methodology for assigning source quantities to the proposed 6 GHz band RLANs and their operating parameters.

3.1 RLAN Deployment Assumptions

3.1.1 Number of Active RLANs and Deployment Distribution

Table 3-1 depicts the parameters and calculations used to develop the numbers of active RLANs. As noted above, this study applies to all RLAN classes below, including but not limited to Wi-Fi Access Points (AP) and stations:

- Indoor (98%):
 - LPI and Standard-Power (88%)¹²
 - VLP (10%)
- Outdoor (2%):
 - Standard-Power (1%)
 - VLP (1%)

At a first level, the deployment of RLANs is assumed to be closely associated with population density, and therefore geographically allocated according to the population distribution in Mexico. The basis of the active device analysis is an estimated Mexico population of 141 million in 2025. As described in Section 3.1.2, we used USCB population density thresholds that determined the percentage of population in urban, suburban, and rural areas across Mexico.

¹² The MSS gateway study will separate out the number of LPI (and LPI clients) and indoor Standard Power (and Standard Power clients) units in order to derive the total number of LPI and Standard Power devices. The total number of indoor versus outdoor devices remains the same.

Table 3-1 - RLAN Active Device Distribution

	TOTAL	URBAN			SUBURBAN			RURAL (includes BARREN)		
Population (%)	100.0000%	77.0%			3.7%			19.3%		
User Type	All	Corporate	Public	Home	Corporate	Public	Home	Corporate	Public	Home
Type (%)	All	10	5	85	5	5	90	2	1	97
Device Population	433,018,636	33,344,470	16,672,235	283,427,997	790,831	790,831	14,234,951	1,675,150	837,575	81,244,771
High Activity Device Population (% of Total)		10%	10%	10%	10%	10%	10%	10%	10%	10%
Data per device per hour, (MBytes)		1000	500	2000	1000	500	2000	1000	500	2000
Device Rate (Mbps)		2.22	1.11	4.44	2.22	1.11	4.44	2.22	1.11	4.44
Link Speed (Mbps)		1000	1000	1000	1000	1000	1000	1000	1000	1000
Duty Cycle per Device		0.22%	0.11%	0.44%	0.22%	0.11%	0.44%	0.22%	0.11%	0.44%
Instantaneous Number of Transmitting 6 GHz Devices (Subtotal, High Activity)	178,395	7,410	1,852	125,968	176	88	6,327	372	93	36,109
Low Activity Device Population (% of Total)		90%	90%	90%	90%	90%	90%	90%	90%	90%
Data per device per hour, (Mbytes)		1	1	1	1	1	1	1	1	1
Device Rate (Mbps)		0.0022	0.0022	0.0022	0.0022	0.0022	0.0022	0.0022	0.0022	0.0022
Link Speed (Mbps)		1000	1000	1000	1000	1000	1000	1000	1000	1000
Duty Cycle per Device		0.00022%	0.00022%	0.00022%	0.00022%	0.00022%	0.00022%	0.00022%	0.00022%	0.00022%
Instantaneous Number of Transmitting 6 GHz Devices (Subtotal, Low Activity)	866	67	33	567	2	2	28	3	2	162
Instantaneous Number of Transmitting 6 GHz Devices (total)	179,261	7,477	1,886	126,535	177	89	6,355	376	95	36,271

Assuming an average RLAN device count of 10 per person, the total RLANs in operation over Mexico is estimated to be 1.41 billion in 2025 and the market penetration of 6 GHz capable RLANs is assumed to be 45%. Because 6 GHz capable RLANs are expected to also operate in the 2.4 and 5 GHz bands, and assuming spectrum loading will be even across all the contemplated channels in the unlicensed bands, 68% of 6 GHz enabled RLANs are estimated to be using the 6 GHz band. As shown in the following equation, the resulting number of RLANs connected to a 6 GHz network is 433 million:

$$\text{Total 6 GHz Attached Devices} = \text{Total Population (people)} \times \text{Devices per Person} \times \text{Market Penetration} \times (\text{target 6 GHz Spectrum}) / (\text{total 2.4 + 5 + 6 GHz Spectrum}) \quad (3-1)$$

$$\text{Total 6 GHz Attached Devices} = (141,132,000 \times 10 \times 0.45 \times 1200/1760) = 433 \text{ Million} \quad (3-2)$$

To estimate indoor versus outdoor deployments, we used Figure 3-2 which depicts the ratio of indoor vs outdoor Wi-Fi AP shipments from 2011 to 2021, including both historical actual shipment figures for Wi-Fi APs through 2016 as well as a forecast for future years. Outdoor unit shipments in 2021 are estimated at 0.6% of all Wi-Fi APs.

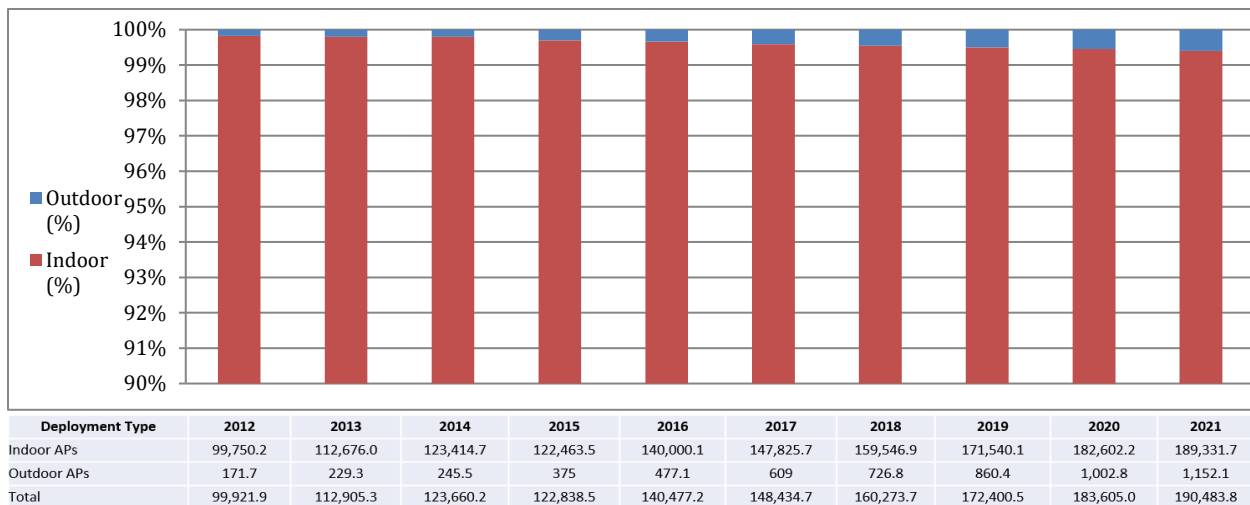


Figure 3-1 - Worldwide Indoor vs Outdoor Wi-Fi Shipments.

Source: Dell'Oro Group July 2017 Wireless LAN report

While this study considers RLANs generally, a conservative model for outdoor 6 GHz RLANs may consider both Wi-Fi and 3GPP based technologies such as Licensed Assisted Access (LAA) because many small cell deployments are expected to be outdoors. Table 3-2 depicts data from the Small Cell Forum and shows a forecast of 1.5 million outdoor small cells deployed in 2021.¹³

Applying the same 45% market penetration for outdoor small cells that are LAA and 6 GHz-capable, yields figures slightly lower than the outdoor Wi-Fi AP market. The combined forecast of Wi-Fi and small cell outdoor shipments is approximately 1% of total units in 2021. Doubling this figure yields a conservative ratio for indoor vs. outdoor RLANs in all sub-markets of 98% and 2% respectively.¹⁴

Table 3-2 - Small Cell Forum Forecast for Outdoor Small Cell Shipments (thousands)

	2014	2015	2016	2017	2018	2019	2020	2021	CAGR
Indoor	176	310	794	1,080	1,901	2,946	3,420	3,239	52%
Outdoor	47	78	251	441	937	1,387	1,466	1,596	66%
Total	223	388	1,045	1,521	2,838	4,333	4,886	4,835	55%

For the peak usage analysis (busy hour), an activity level was assigned to represent the amount of data consumed wirelessly. For this analysis, the activity on these RLANs was distributed around two primary modes (i.e., bi-modal):

- “High activity” mode – Typical of RLANs in active use by a person. For this simulation we assumed one device per person, a more conservative model than typical assumptions.

¹³ This data is based on a forecast made in 2018.

¹⁴ 5G Americas and Small Cell Forum, *Multi-operator and Neutral Host Small Cells: Drivers, Architectures, Planning and Regulation*, Dec. 2016, http://www.5gamerica.org/files/4914/8193/1104/SCF191_Multi-operator_neutral_host_small_cells.pdf.

- “Low activity” mode – Typical of RLANs making periodic or intermittent transfers of data, such as RLANs connected to the network but not in direct use (idle), or RLANs that make small data transfers typical of “Internet of Things” (IoT) connected devices.

To determine the worst-case time of interference into incumbent systems, busy hours for corporate, public, and home usage were studied. The study assumed that RLAN usage is heaviest during busy hour across Mexico of 7:00 pm – 8:00 pm CDMX. It was assumed that on average every person in Mexico is actively using one RLAN during the busy hour while owning an average of nine other RLANs that were not being actively used. As a result, the percentage of devices in the High activity mode was assumed to be 10% and 90% were assumed to be in the Low activity mode.^{15,16}

For devices in the High activity mode, usage was modeled to be 2.0 Gbytes/hour (4.44 Mbps) for the home user, 1 Gbytes/hour (2.22 Mbps) for the corporate user, and 500 Mbytes/hour (1.11 Mbps) for public (hotspot connected) users. For devices in the Low activity mode, usage was modeled to be 1 Mbyte/hour (2.2 kbps).

As a final step in this derivation, the efficiency of high bitrate modulation techniques offered by modern unlicensed wireless technologies is considered. It is expected that new, 6 GHz technology will deliver an average application layer throughput rate of 1 Gbps as achieved in current 5 GHz technology. It is also expected that this capability will be deployed for the types of 6 GHz devices in use during the busy hour for applications like video streaming. Based on the available over-the-air rate of the AP, the data required per device per hour and the required duty cycle can be assigned per device as follows:

$$\text{Device Duty Cycle} (\% \text{ of available airtime}) = \frac{\text{Data per Device per Hour (Mbytes)} \times (8 \text{ bits / 3600 secs})}{\text{Average Rate (Mbps)}} \quad (3-3)$$

For example, for the Home Market active device model

$$\text{Device Duty Cycle} = 2000 \text{ MBytes} \times (8/3600) / 1000 \text{ Mbps} = 0.44 \% \quad (3-4)$$

The number of instantaneously active devices included in the model over all of Mexico is the sum of the low and high activity mode devices for all markets (urban, suburban, rural) and environments (corporate, public, home) as follows:

$$\text{Instantaneous Transmitting Devices} = \text{Total Devices Using 6 GHz} \times \text{Duty Cycle} \quad (3-5)$$

Note that the device duty cycle is calculated and assigned for all RLANs in each of the above market types and environments and for both low and high activity mode devices. Table 3-1 shows the resulting input quantities of instantaneous transmitting devices for each of these markets and environments.

¹⁵ ITU document Revision 1 to 5A/TEMP/236, Sharing and compatibility studies of WAS/RLAN in the 5 150-5 250 MHz frequency range, Section 5.1.1.4.2.5, stated busy hour demographic factor was 71%, 64%, and 47% for urban suburban, and rural populations. This simulation assumed 90%.

¹⁶ While the ITU-R Working Party 5A concludes that busy hour participation is 62.7%, this simulation uses 90%. ITU-R, *Annex 22 to Working Party 5A Chairman’s Report: Use of Aggregate RLAN Measurements from Airborne and Terrestrial Platforms to Support Studies Under WRC-19 Agenda Item 1.16* (Nov. 16, 2017) at 3, available at <https://www.itu.int/md/R15-WP5A/new/en> (ITU-R 5A/650 (Annex 22)-E).

3.1.2 Population Density

Sharing analysis for this report used an estimated 2025 population density, based on the UN World Population Prospects, to randomly distribute the active RLANs estimated in Section 3.1.1.¹⁷ Population density thresholds, were derived over the contiguous United States (CONUS) by dividing CONUS into 71.2% urban, 9.5% suburban, and 19.3% rural¹⁸ geo areas, based on USCB 2010 percentages. This resulted in population density thresholds that are applied to Mexico's population density grid database per below:

- if population density \geq people/km², it is urban;
- else if 227.30449 people/km² \leq population density $<$ 513.04217 people/km², it is suburban;
- else, it is rural.

This resulted in percentages of Mexico population and area in urban, suburban and rural geo-areas per Table 3-3.

The resulting population and area percentages shown in Table 3-1 were used in the simulations to randomly distribute the number of RLANs estimated in Section 3.1.1 for sharing analysis with the existing uplink FSS and FS services, and the future MSS gateway in the 6 GHz band.

As can be seen, approximately 98% of Mexico is rural, which implies that interference will be predominantly concentrated in urban and suburban areas.

Table 3-3 - Population Density in Mexico

	Population (%)	Area¹⁹ (%)
Urban	77.0%	1.4%
Suburban	3.7%	0.8%
Rural	19.3%	97.7% ²⁰

3.2 RLAN Operating Assumptions

To perform a thorough simulation of RLAN sharing of the 6 GHz band, reasonable statistical operating assumptions were developed to account for the myriad possibilities of RLAN use given the deployment models in Section 3.1. As described in that section, we are considering rural, suburban, and urban environments with corporate, public, and home submarkets. Within each of these nine submarkets, key operating parameters that affect the received interference level include RLAN source EIRP, bandwidth and channel usage, and installed height. Because

¹⁷ Socioeconomic Data and Applications Center, *Gridded Population of the World (GPW)*, v4, NASA, <http://sedac.ciesin.columbia.edu/data/collection/gpw-v4/maps/gallery/search?facets=theme:population> (last visited June 27, 2020).

¹⁸ These definitions are consistent with the 2010 Census Bureau classifications (urban clusters, urbanized areas, and rural environments).

¹⁹ The sum of the areas does not add to 100% due to rounding.

²⁰ 10.6% of the area has zero population.

these operating parameters can vary, statistical assumptions must be derived before they can be used in the simulations.

3.2.1 Distribution of Source LPI and Standard Power with AFC RLAN Power Levels

To develop the statistical LPI and Standard Power with AFC RLAN source power, or EIRP, we looked at typical use cases, RLAN peak power, and busy hour usage weights for LPI and Standard Power with AFC RLANs (referred to “RLANs” in this section). Since RLAN locations and antenna orientations tend to be random and RLANs generally have a wide range of available output power and operating characteristics, randomization of the RLAN source EIRP values is a valid approach for the broad statistical analysis of this report.

As stated in Section 3.1, both indoor and outdoor RLAN installations were randomized based on population density and therefore can be installed anywhere relative to a victim receiving location. In each installation, the orientation of the RLAN antenna is in general not fixed. Therefore, in the analysis we assumed an equal weight assigned to all values in the E-plane pattern. Outdoor RLAN antennas most likely will be oriented such that the omnidirectional pattern is horizontal with respect to the ground at the installation site and, as shown in Figures 3-4 through 3-9, will be designed to limit maximum EIRP to 1 Watt above 30° in elevation (9 dB higher than currently allowed in U-NII-1 rules). Even though indoor RLAN antennas have similar elevation patterns (E-plane) as outdoor RLANs, an isotropic radiating pattern for all indoor RLANs was used in the simulations to define a worst-case scenario.

Given these basic assumptions, the expected RLAN power levels can be represented by a distribution of power levels. To derive the RLAN source EIRP in the submarkets described in Section 3.1.1, seven typical use cases were used.

- Indoor Enterprise AP, Indoor Consumer AP, and Indoor High-Performance AP
- Indoor/Outdoor Client
- Outdoor High-Power AP, Outdoor Low Power AP

Table 3-4 provides the peak power of these use cases in the elevation patterns (E-plane) depicted in Figure 3-3 through 3-8. For this analysis, the horizontal patterns (H-plane) were assumed to be omnidirectional.

Table 3-4 – Peak Power (EIRP) of Typical LPI and Standard Power with AFC RLAN Use Cases

	Indoor Enterprise AP	Indoor Consumer AP	Indoor High Performance Gaming Router	Indoor/Outdoor Client	Outdoor High Power AP	Outdoor Low Power AP
	<i>Figure 3-4</i>	<i>Figure 3-5</i>	<i>Figure 3-6</i>	<i>Figure 3-7</i>	<i>Figure 3-8</i>	<i>Figure 3-9</i>
Conducted Power (dBm)	13.5	12.5	24	12	27	14
Peak Antenna Gain (dBi)	4.1	5.3	5.3	3.5	5.3	5.3
MIMO Gain (dB)	6.0	6.0	6.0	3.0	3.0	4.8
Total Peak EIRP (dBm)	23.6	23.8	35.3	18.5	35.3	24.1

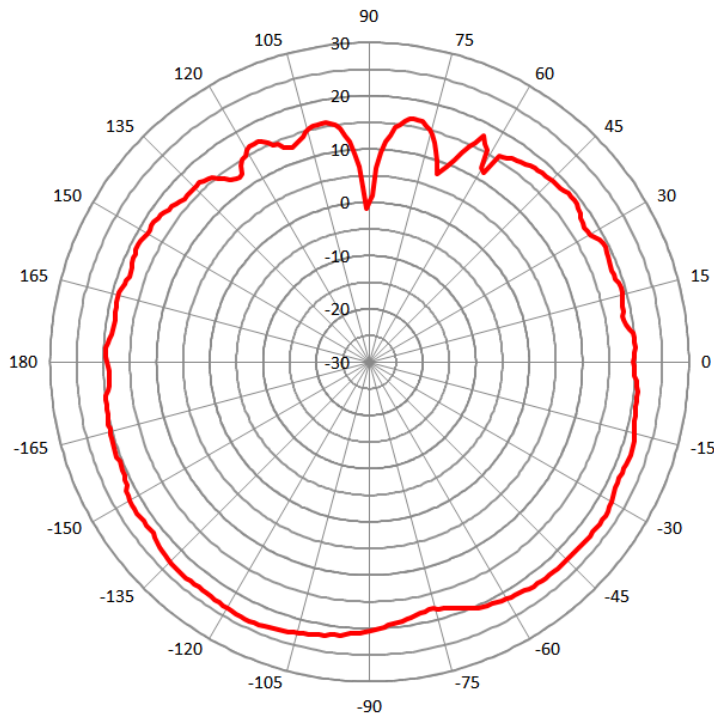


Figure 3-2 - Indoor Enterprise Access Point, Typical Pattern (EIRP)

Indoor Enterprise Access Point EIRP Probability based on E-Plane Directivity	
$36 \text{ dBm} \leq 30 \text{ dBm}$	0.00%
$< 30 \text{ dBm} \leq 24 \text{ dBm}$	0.00%
$< 24 \text{ dBm} \leq 20 \text{ dBm}$	40.17%
$< 20 \text{ dBm} \leq 17 \text{ dBm}$	34.07%
$< 17 \text{ dBm} \leq 11 \text{ dBm}$	22.16%
$< 11 \text{ dBm} \leq 0 \text{ dBm}$	3.32%
$< 0 \text{ dBm}$	0.28%
Total	100.00%

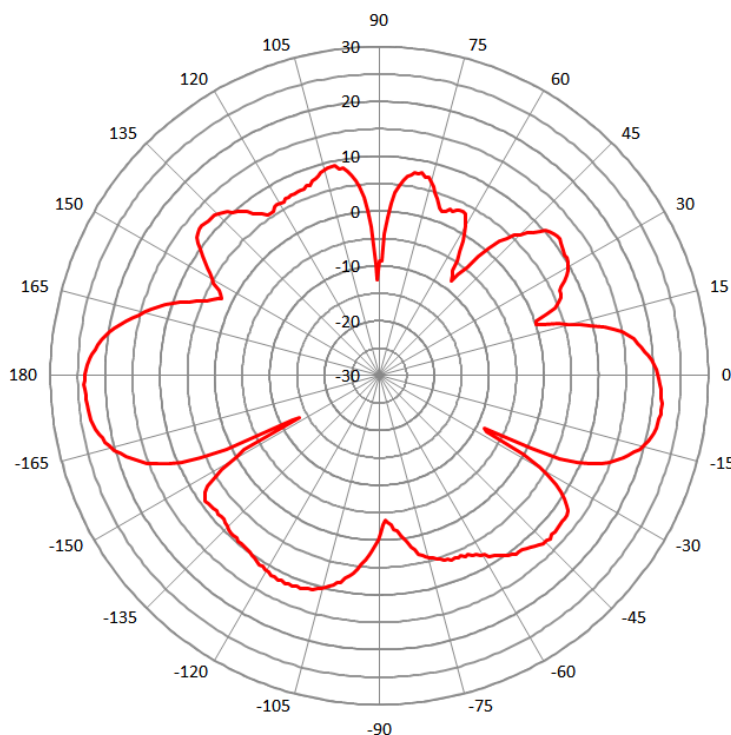


Figure 3-3 - Indoor Consumer Access Point, Typical Pattern (EIRP)

Indoor Consumer Access Point EIRP Probability based on E-Plane Directivity	
$36 \text{ dBm} \leq 30 \text{ dBm}$	0.00%
$< 30 \text{ dBm} \leq 24 \text{ dBm}$	0.00%
$< 24 \text{ dBm} \leq 20 \text{ dBm}$	11.19%
$< 20 \text{ dBm} \leq 17 \text{ dBm}$	4.16%
$< 17 \text{ dBm} \leq 11 \text{ dBm}$	16.90%
$< 11 \text{ dBm} \leq 0 \text{ dBm}$	58.73%
$< 0 \text{ dBm}$	8.31%
Total	100.00%

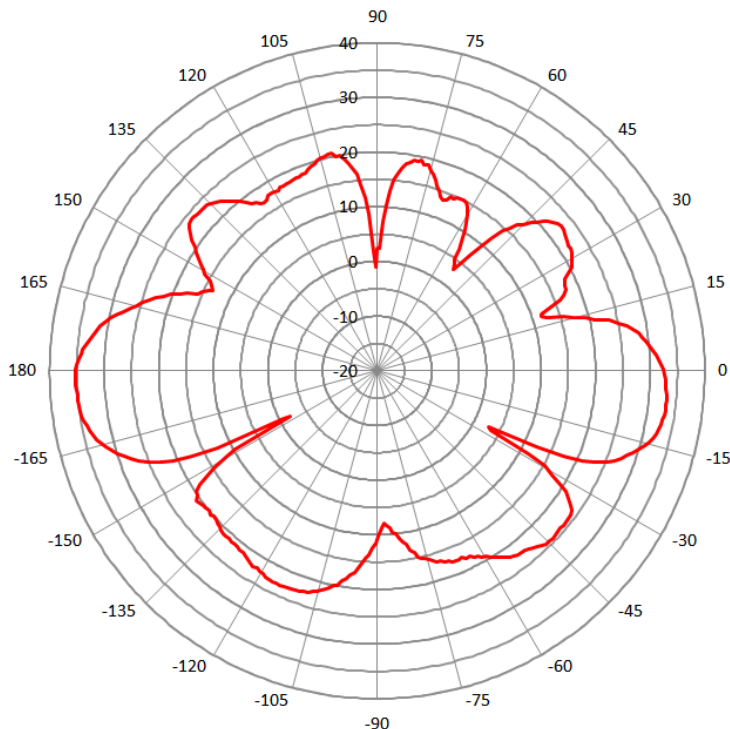


Figure 3-4 - Indoor High-Performance Gaming Router, Typical Pattern (EIRP)

**Indoor High-Performance
Gaming Router Access Point**
EIRP Probability based on E-
Plane Directivity

36 dBm \leq 30 dBm	14.13%
< 30 dBm \leq 24 dBm	8.86%
< 24 dBm \leq 20 dBm	30.19%
< 20 dBm \leq 17 dBm	21.33%
< 17 dBm \leq 11 dBm	17.45%
< 11 dBm \leq 0 dBm	7.20%
< 0 dBm	0.83%
Total	100.00%

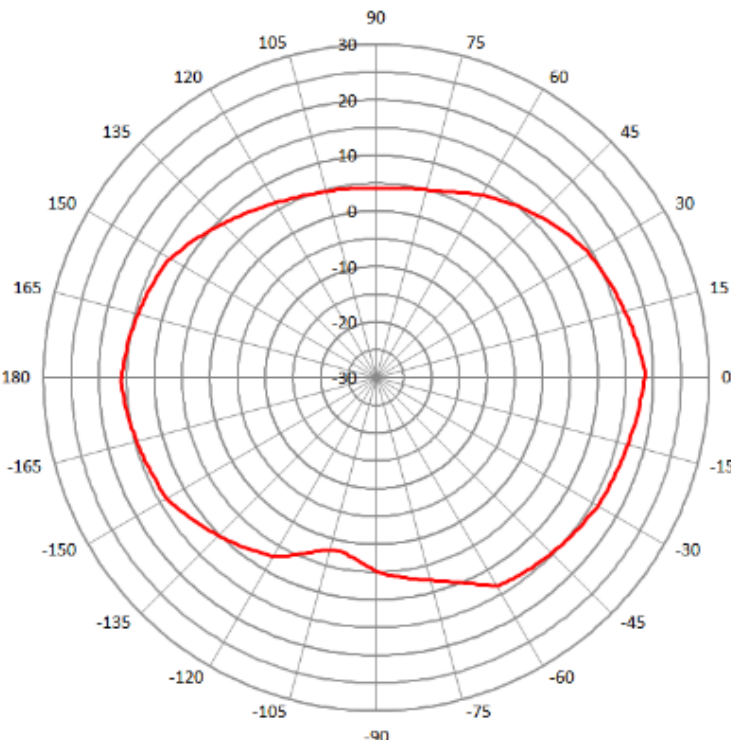


Figure 3-5 - Indoor and Outdoor Client, Typical Pattern (EIRP)

Indoor and Outdoor Client
EIRP Probability based on E-
Plane Directivity

36 dBm \leq 30 dBm	0.00%
< 30 dBm \leq 24 dBm	0.00%
< 24 dBm \leq 20 dBm	0.00%
< 20 dBm \leq 17 dBm	6.93%
< 17 dBm \leq 11 dBm	45.71%
< 11 dBm \leq 0 dBm	47.37%
< 0 dBm	0.00%
Total	100.00%

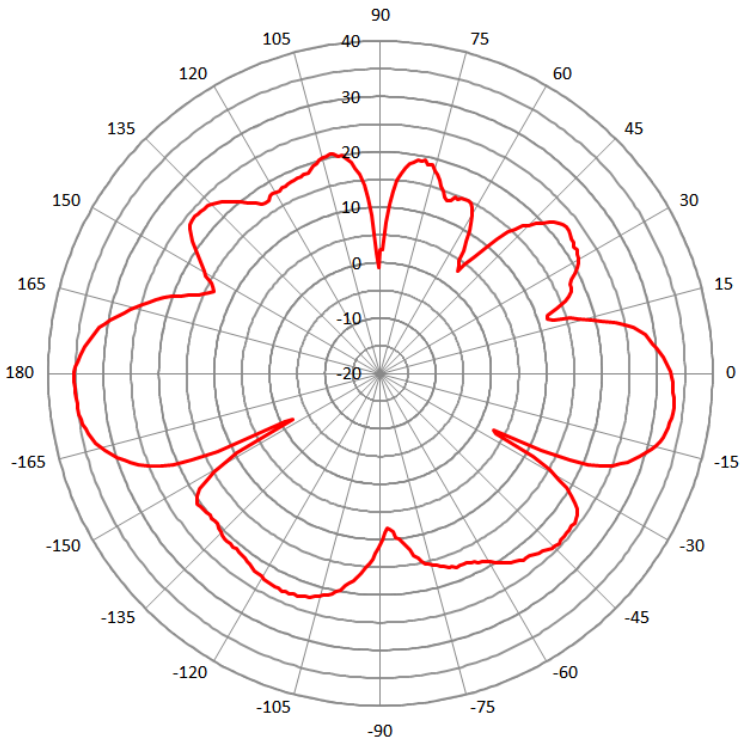


Figure 3-6 - Outdoor High-Power Access Point, Typical Pattern (EIRP)

Outdoor High-Power Access Point EIRP Probability based on E-Plane Directivity	
36 dBm \leq 30 dBm	14.13%
< 30 dBm \leq 24 dBm	8.86%
< 24 dBm \leq 20 dBm	30.19%
< 20 dBm \leq 17 dBm	21.05%
< 17 dBm \leq 11 dBm	17.73%
< 11 dBm \leq 0 dBm	7.20%
< 0 dBm	0.83%
Total	100.00%

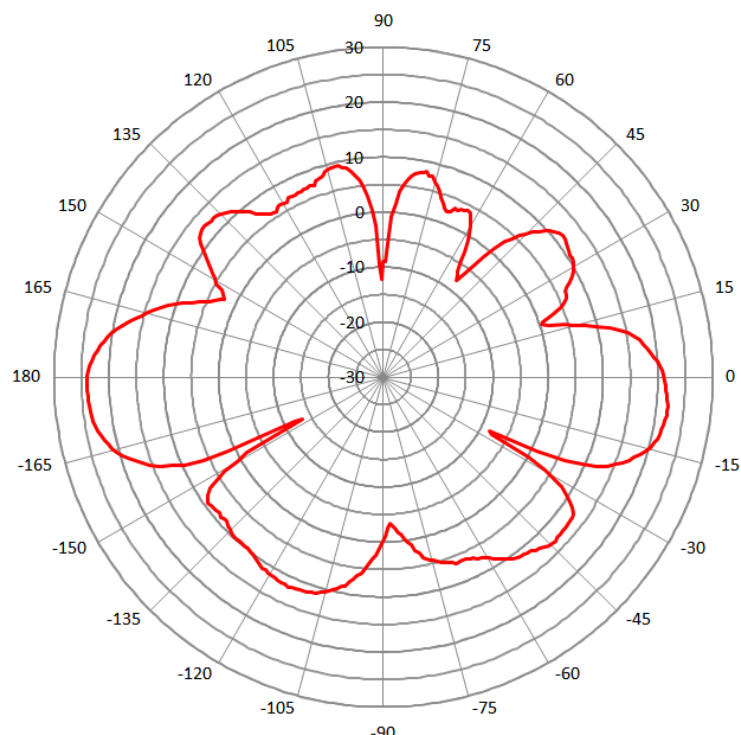


Figure 3-7 - Outdoor Low-Power Access Point, Typical Pattern (EIRP)

Outdoor Low Power Access Point EIRP Probability based on E-Plane Directivity	
36 dBm \leq 30 dBm	0.00%
< 30 dBm \leq 24 dBm	0.83%
< 24 dBm \leq 20 dBm	11.36%
< 20 dBm \leq 17 dBm	4.43%
< 17 dBm \leq 11 dBm	19.11%
< 11 dBm \leq 0 dBm	56.23%
< 0 dBm	8.03%
Total	100.00%

The mix of indoor and outdoor RLANs is conservatively estimated at 98% and 2%, respectively (Section 3.1.1). Table 3-5 provides busy hour weights for indoor use cases. Note that device weights correspond to a 1:1 ratio of downlink to uplink traffic for corporate and public users, and a 2.3:1 ratio for home users.

Table 3-5 - Busy Hour Weights Assigned to Use Cases, Indoor Environments (by submarket)

User Type	URBAN			SUBURBAN			RURAL			BARREN		
Client	50%	50%	25%	50%	50%	25%	50%	50%	25%	50%	50%	25%
Enterprise AP	50%	50%	0%	50%	50%	0%	50%	50%	0%	50%	50%	0%
Consumer AP	0%	0%	70%	0%	0%	70%	0%	0%	70%	0%	0%	70%
High-Performance Gaming Router	0%	0%	5%	0%	0%	5%	0%	0%	5%	0%	0%	5%
Total (Indoor)	100											

Since outdoor RLAN usage is not expected to vary significantly by submarkets, all use cases were assigned the same weights in all submarkets (Table 3-6) and, for all outdoor scenarios, a 1:1 ratio of downlink to uplink traffic was used.

The combination of the use case busy hour weights of Tables 3-5 and 3-6, with the E-plane patterns shown in Figures 3-4 through 3-9, results in a power distribution for the source RLANs as shown in Table 3-7 for indoor RLANs and Table 3-8 for outdoor RLANs. This results in weighted average EIRPs for indoor RLANs of 19.167 dBm, outdoor RLANs of 22.73 dBm, and combined indoor/outdoor of 19.28 dBm are used in the simulations. It is noted that although these weighted average EIRP values were independently derived by the methods described above, the resulting values are consistent and slightly conservative compared to EIRP values used for previous RLAN sharing studies.^{21,22,23}

Table 3-6 - Busy Hour Weights Assigned to Use Cases, Outdoor Environment (all sub-markets)

	URBAN	SUBURBAN	RURAL
Outdoor High-Power AP (Figure 3-8)	20%	20%	20%
Outdoor Low Power AP (Figure 3-9)	30%	30%	30%
Outdoor Client (Figure 3-7)	50%	50%	50%
Total (Indoor)	100%	100%	100%

The distributions in Tables 3-7 and 3-8 represent the probability of the specified EIRP occurring in any random direction from an active RLAN. For the purposes of simulation, the continuous values in between each breakpoint shown in the tables are represented as the maximum value. For example, the probability of a 250 mW EIRP from Table 3-7 for indoor RLANs of 10.39% is inclusive of all continuous EIRP probabilities greater than 100 mW, up to and including 250 mW, and were then

²¹ ITU document Revision 1 to 5A/TEMP/236, Sharing and compatibility studies of WAS/RLAN in the 5 150-5 250 MHz frequency range, Section 5.1.1.4.2.1, average EIRP is 18.9 dBm for indoor RLANs, 21.2 dBm for outdoor RLANs, and 19 dBm for indoor and outdoor.

²² ITU document Revision 1 to 5A/TEMP/236, Sharing and compatibility studies of WAS/RLAN in the 5 150-5 250 MHz frequency range, Appendix 2, Section 5.1.4.2.1, states average power used in the analysis was 19 dB with average.

²³ The ITU-R concludes that a mean EIRP of 19 dBm should be used for 5 GHz RLAN studies. ITU-R 5A/650 (Annex 22)-E at 3.

included in the simulation as 250 mW sources with a 10.39% probability of occurrence. Because the distributions of Tables 3-7 and 3-8 already assume the RLAN antenna orientation to the victim receive locations are random, no further adjustment is provided in the analysis for directivity effects of the RLAN sources. This is equivalent to stating that the above EIRP values are treated isotropically (radiate equally in all directions) once seeded into the model for a given source location. EIRP values above 1W up to and including 4W are modeled as isotropic for indoor use cases, but limited (truncated) to 1W at elevation angles above 30° for outdoor RLANs as described above.

Table 3-7 - LPI and Standard Power with AFC Indoor Source EIRP Distribution (mW)

Indoor Use Case	Weight	Weighted EIRP Distribution (mW)								Total
		4000	1000	250	100	50	13	1		
Client	26.32%	0.00%	0.00%	0.00%	1.82%	12.03%	12.47%	0.00%	26.32%	
Enterprise AP	2.63%	0.00%	0.00%	1.06%	0.90%	0.58%	0.09%	0.01%	2.63%	
Consumer AP	66.31%	0.00%	0.00%	7.90%	2.76%	11.20%	38.94%	5.51%	66.31%	
High-Performance Gaming Router	4.74%	0.67%	0.42%	1.43%	1.01%	0.83%	0.34%	0.04%	4.74%	
Sub-Total	100.00%	0.67%	0.42%	10.39%	6.49%	24.64%	51.84%	5.56%	100.00%	

The weights shown in Table 3-7, that applies to LPI and Standard-Power Indoor devices, were obtained by combining the use cases of Table 3-5 with the active device populations shown in Table 3-1. For example, the indoor client weight of 26.32% is obtained as the weighted sum of the active devices inclusive of all submarkets as derived in the equation below.

$$\text{Indoor Client Weight} = \{\text{Table 3-5 [Urban (Corporate, Public, Home)]} \times \text{Table 3-1 Device Population [Urban (Corporate, Public, Home)]} + \text{Table 3-5 [Suburban (Corporate, Public, Home)]} \times \text{Table 3-1 Device Population [Suburban (Corporate, Public, Home)]} + \text{Table 3-5 [Rural (Corporate, Public, Home)]} \times \text{Table 3-1 Device Population [Rural (Corporate, Public, Home)]}\} / \{\text{Table 3-1 [Total Active Devices]}\} \quad (3-6)$$

The weights shown in Table 3-8, that applies to Outdoor Standard-Power devices, are the same as Table 3-6 for all outdoor devices because there is no variation assumed in the proportion of active devices for each use case across the sub-markets.

Table 3-8 – Outdoor Standard Power with AFC RLAN Source EIRP Distribution (mW)

Outdoor Use Case	Weight	Weighted EIRP Distribution (mW)								Total
		4000	1000	250	100	50	13	1		
High Power AP	20%	2.83%	1.77%	6.04%	4.21%	3.55%	1.44%	0.17%	20.00%	
Low Power AP	30%	0.00%	0.25%	3.41%	1.33%	5.73%	16.87%	2.41%	30.00%	
Client	50%	0.00%	0.00%	0.00%	3.46%	22.85%	23.68%	0.00%	50.00%	
Sub-Total	100.00%	2.83%	2.02%	9.45%	9.00%	32.13%	41.99%	2.58%	100%	

For the simulation, interference results are presented as the aggregate interference from a deployment of all RLAN device types.

3.2.2 Body Loss for LPI and Standard Power with AFC Indoor and Outdoor devices

RF signal attenuation that is caused by the human body is typically taken into account in sharing studies with mobile client devices. A fixed body loss value of 4 dB is applied when the modelled LPI or Standard Power with AFC RLAN device is a client, while body loss is assumed to be non-existent for Access Point devices. The percentage of client devices is given as 26.32% and 50% for indoor and outdoor deployments, respectively, in Section 3.2.1. Hence, the following methodology is applied in the Monte-Carlo simulations for LPI and indoor and outdoor Standard Power with AFC devices:

- For indoor devices, apply 4 dB additional loss for 26.32% of the devices (clients)
- For outdoor devices, apply 4 dB additional loss for 50% of the devices (clients)

3.2.3 Distribution of Source VLP Power Levels including Body Loss

For VLP devices where the body interacts with the device (because the device is closer to body), for higher accuracy, the full distribution of body loss is used. Antenna gain measurements were made in proximity of the human body considering various use case device positioning, static vs. dynamic conditions, device orientations, and the physical characteristics of the human body. The comprehensive on-body over-the-air measurements and analysis of the associated body loss distributions applicable to the indoor and outdoor VLP device are described in the Wireless Research Center of North Carolina study attached to the RLAN Group Comments, and shown in Figure 3-8.²⁴ In the Monte-Carlo simulations, antenna gain values ($G_{FarField}$ in Eqn. 2-1) are selected randomly from the distribution in Figure 3-8 and is added to a fixed value of 14 dBm to get the net EIRP level that includes antenna mismatch and body loss for indoor and outdoor VLP devices.

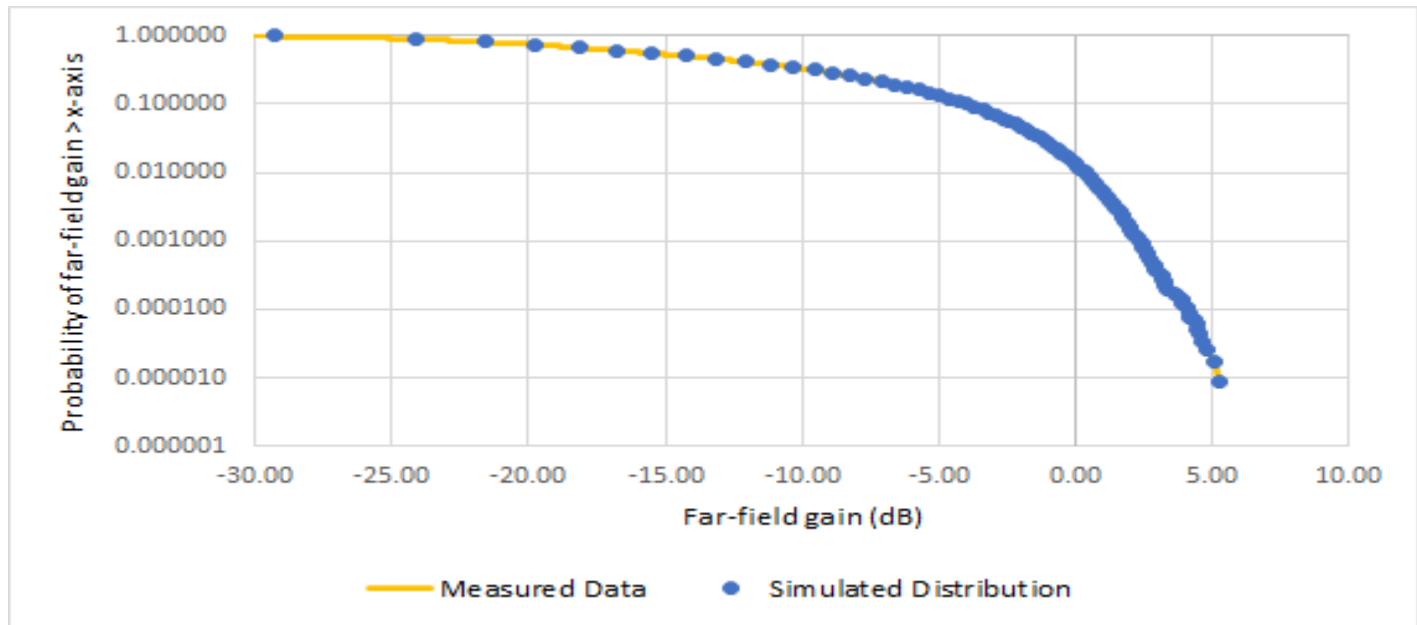


Figure 3-8 – Probability of VLP device far-field gain $>$ x-axis: measurements versus simulated distribution

²⁴ Wireless Research Center of North Carolina, On-Body Channel Model and Interference Estimation at 5.9 GHz to 7.1 GHz Band at Fig. 26 (June 2020).

3.2.4 Bandwidth and Channel Distribution

RLANs modeled in this report are assumed to operate in 20 MHz, 40 MHz, 80 MHz, and 160 MHz bandwidth channels. To determine the number of channels, and how those channels may overlap with FSS and FS receivers, the following channel plan outlined in Figure 3-9 was assumed. Note that the 20-MHz channel from 5925-5945 MHz (channel index 2) was not included in the model.

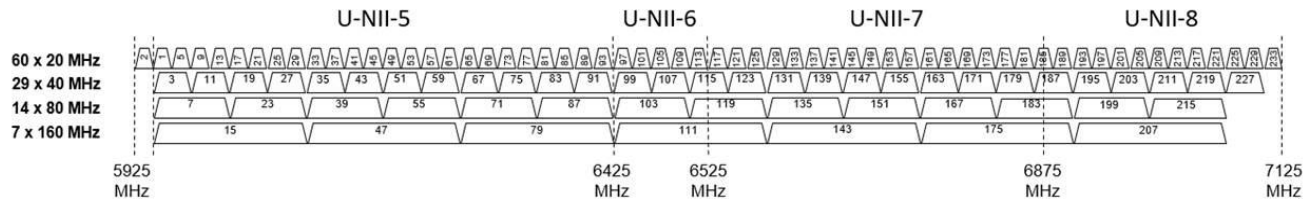


Figure 3-9 - Assumed RLAN Channel Plan

The bandwidth distribution in Table 3-9 is based on the assumption that RLAN systems will operate with larger channel sizes to maximize airtime efficiency, resulting in lower latency, higher throughput, and improved battery life.

Table 3-9 – RLAN Channel Distribution

Bandwidth	20 MHz	40 MHz	80 MHz	160 MHz
Percentage	10%	10%	50%	30%

3.2.3 Distribution of RLAN heights

Outdoor VLP devices are worn on mobile users, and a large majority of these use cases are with the VLP device below 1.5 m.

To assign an RLAN transmit source height to the remaining RLAN classes (i.e., LPI, indoor VLPs and indoor/outdoor Standard Power with AFC devices (here-in after referred to “RLANs” in this section), a height distribution was separately prepared for each of the following indoor environments: urban, suburban, and rural. In addition, a common outdoor height distribution was used for all environments. The starting point of the height distribution is the building construction type probability for each environment, shown in Table 3-10.²⁵

Within multi-story buildings, the distribution of RLANs is assumed to have an equal probability of occurring on any floor up to ten stories. A height of ten stories was selected as the maximum because the probability of RLANs on higher floors diminishes significantly even when taller buildings are considered. Stated differently, studying taller buildings does not impact the analysis in any significant way. This is due to the assumed equal spreading of RLANs on all floors of a tall building, which results in the combined distribution being heavily weighted toward lower floors.

²⁵ U.S. Energy Info. Admin., 2012 Commercial Buildings Energy Consumption Survey: Building Questionnaire - Form EIA-871A, <https://www.eia.gov/consumption/commercial/data/2012/pdf/questionnaire.pdf>; NAHB, *The Number of Stores in Single-Family Homes Varies Across the Country*, Aug. 5, 2016, <http://eyeonhousing.org/2016/08/the-number-of-stories-in-single-family-homes-varies-across-the-country/>.

For example, the 28.5m height assumed for RLANs on the 10th floor of a ten-story building comprises only 0.02% of all RLANs in the Urban environment. It is noted that the inclusion of the 10-story building in the analysis, while placing 0.02% of RLANs at this height, increases

Table 3-10 - Building Construction Type Probability by Environment

		Urban Indoor			Suburban Indoor			Rural Indoor			Outdoor
Building Story	Height (m)	Corp	Public	Home	Corp*	Public	Home	Corp	Public	Home	
1	1.5	69.0%	69.0%	60.0%	69.0%	69.0%	60.0%	70%	70%	70%	95%
2	4.5	21.0%	21.0%	30.0%	21.0%	21.0%	30.0%	25%	25%	25%	2%
3	7.5	7.0%	7.0%	7.0%	7.0%	7.0%	5%	5%	5%	5%	2%
4	10.5	0.7%	0.7%	0.7%	0.7%	0.7%	5%	0%	0%	0%	0.5%
5	13.5	0.58%	0.6%	0.6%	0.58%	0.6%	0%	0%	0%	0%	0%
6	16.5	0.50%	0.5%	0.5%	0.50%	0.5%	0%	0%	0%	0%	0%
7	19.5	0.43%	0.4%	0.4%	0.43%	0.4%	0%	0%	0%	0%	0%
8	22.5	0.35%	0.4%	0.4%	0.35%	0.4%	0%	0%	0%	0%	0%
9	25.5	0.28%	0.3%	0.3%	0.28%	0.3%	0%	0%	0%	0%	0%
10	28.5	0.2%	0.2%	0.2%	0.2%	0.2%	0%	0%	0%	0%	0.5%
Total		100.00	100.00	100.00	100.00	100.00	100.00	100.00	100.00	100.00	100.00

the probability of RLANs at heights on floors one through nine by 10% of the ten-story building type probability. For example, the likelihood that an RLAN will be on the first floor in an urban environment is the sum as follows:

$$\begin{aligned} \text{RLAN on 1}^{\text{st}} \text{ Floor Probability} &= 1 \text{ Story Building Probability} + 2 \text{ Story Building Probability}/2 Floors \\ &\dots + 10 \text{ Story Building Probability}/10 Floors \end{aligned} \quad (3-7)$$

As such, including buildings of taller heights provides limited additional insight into the question of aggregated RLAN interference because each additional building height of n stories that is included provides only a $1/n$ contribution to the distribution of RLANs at that height, while the rest are distributed as $1/n$ to each of the lower floors.

Using the above described method based on the building construction type probability and equal assignment of RLANs to each floor of a multi-story building results in the distribution of source heights shown in Table 3-11.

Table 3-11 - RLAN Source Height Distributions

		Urban Indoor			Suburban Indoor			Rural Indoor			Outdoor
Building Story	Height (m)	Corp	Public	Home	Corp*	Public	Home	Corp	Public	Home	
1	1.5	82.35 %	82.35 %	77.85 %	82.35 %	82.35 %	77.92 %	84.17 %	84.17 %	84.17 %	95.00%
2	4.5	13.35 %	13.35 %	17.85 %	13.35 %	13.35 %	17.92 %	14.17 %	14.17 %	14.17 %	2.00%
3	7.5	2.85%	2.85%	2.85%	2.85%	2.85%	2.92%	1.67%	1.67%	1.67%	2.00%
4	10.5	0.52%	0.52%	0.52%	0.52%	0.52%	1.25%	0.00%	0.00%	0.00%	0.50%
5	13.5	0.36%	0.36%	0.36%	0.36%	0.36%	0.00%	0.00%	0.00%	0.00%	0.00%

6	16.5	0.24%	0.24%	0.24%	0.24%	0.24%	0.00%	0.00%	0.00%	0.00%	0.00%
7	19.5	0.16%	0.16%	0.16%	0.16%	0.16%	0.00%	0.00%	0.00%	0.00%	0.00%
8	22.5	0.09%	0.09%	0.09%	0.09%	0.09%	0.00%	0.00%	0.00%	0.00%	0.00%
9	25.5	0.05%	0.05%	0.05%	0.05%	0.05%	0.00%	0.00%	0.00%	0.00%	0.00%
10	28.5	0.02%	0.02%	0.02%	0.02%	0.02%	0.00%	0.00%	0.00%	0.00%	0.50%
Total		100.00									

4 Propagation Models

The interference paths from a large deployment of RLANs to other services will vary considerably with terrain, local ground clutter, and the location of the RLAN installation (e.g., indoor or outdoor, building heights, building type, density of buildings, etc.). Interference estimates therefore require statistical propagation models that can account for this large variability and random nature of some of the propagation effects.

Section 4.1 describes propagation models used by RKF to calculate path loss for RLAN interference to the FSS. Section 4.2 describes propagation models used to calculate path loss for RLAN interference to terrestrial services. Section 4.3 describes the propagation models used to calculate the path loss for the RLAN interference into the earth station antenna at the MSS gateway.

4.1 RLAN to FSS Propagation Models (Earth to Space)

Figure 4-1 shows possible interference paths from terrestrial sources to satellites on the geosynchronous (GEO) arc. Paths from indoor devices will experience penetration losses through buildings. Some paths will then interact with terrain, while others will suffer from local end-point clutter (e.g., buildings), and still others will have line-of-site (LOS) visibility to the GEO arc.

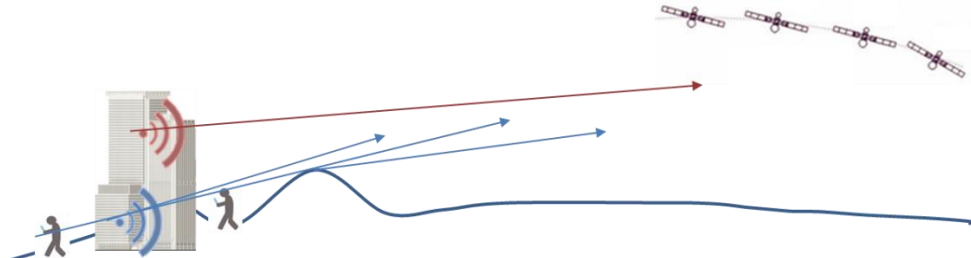


Figure 4-1 - Typical Interference Paths toward the GEO Arc

Figure 4-1 Key	
	Indoor RLAN
	Outdoor RLAN
	LOS Path
	Paths that interact with terrain and/or suffer from end-point-clutter

Paths from indoor RLANs to terrestrial systems experience penetration loss calculated using Recommendation ITU-R P.2109 (P.2109) as the path exits a building. P.2109 is a heuristic model based on many measurements with users located randomly within a building. It considers the elevation angle of the signal leaving the building to the affected receiver. Two types of buildings are defined:

traditional and thermally efficient. Penetration losses through thermally efficient buildings are higher than traditional buildings. The models conservatively assume 80% of buildings are traditional and 20% of buildings are thermally efficient.²⁶

Local end-point clutter is added using Recommendation ITU-R P.2108 (P.2108), Section 3.3 (for Earth-space paths). This is a statistical clutter model for urban and suburban areas. It accounts for the elevation angles from the transmitters to the satellites. According to guidance from ITU-R Study Group 3, the model is currently used only for frequencies above 10 GHz.²⁷ This is because building penetration is not taken into account. However, it is reasonable to assume that at 6 GHz, buildings will be mostly opaque (i.e., large losses will occur transmitting through buildings). This is verified using P.2109 for indoor users, where average penetration loss through traditional buildings at 6 GHz and at an elevation angle of 30° is about 20 dB.

To estimate rural clutter loss, Recommendation ITU-R P.452 (P.452) was used with RLANs deployed predominately in village centers. P.452 assumes that in village centers clutter height is 5 m and the distance to the clutter is 0.07 km which equals an angle of 2.86°. Therefore, in the simulations, when the rural RLAN height is 1.5 m, a clutter loss of 18.4 dB was added when the look angle to the FSS receiver was ≤ 2.86°. When rural RLAN heights are above 1.5m, the clutter loss is assumed to be negligible and is not calculated.

For LOS paths, the radio horizon is defined using 4/3 earth assumptions. Free space path loss is used when there is no blockage from the transmitter to the satellite. Conservatively, atmospheric loss, which is small, was ignored in this calculation.

4.2 RLAN to Terrestrial FS Propagation Models

Possible interference paths from RLANs to terrestrial FS systems are similar to those described in Section 4.1 for paths from terrestrial systems to satellites on the GEO arc, with the addition of a terrain model (as described below). Like Section 4.1, paths from indoor RLANs to terrestrial systems experience penetration loss calculated using P.2109 as the path exits a building.

The Irregular Terrain Model (ITM) model of radio propagation is a general-purpose model for frequencies between 20 MHz and 20 GHz that can be applied to a large variety of engineering problems. The model, which is based on electromagnetic theory and statistical analyses of both terrain features and radio measurements, predicts the median attenuation of a radio signal as a function of distance and the variability of the signal in time and in space. The ITM, along with the Shuttle Radar Topography Model (SRTM) (3 sec) terrain database, is used to model terrain interactions. The ITM uses the SRTM terrain elevation data along with diffraction theory to calculate the path loss when there is terrain blockage.

The analyses use propagation models adopted per the FCC's 6 GHz Report & Order.²⁸ As a function of the separation distance between the RLAN and victim receiver, these models are as follows:

²⁶ Note that in the US, the 6 GHz Report and Order used 70% traditional and 30% thermally-efficient.

²⁷ 5A/337-E, 3 April 2017, Working Parties 3K and 3M, LIAISON STATEMENT TO WORKING PARTY 5A, PROPAGATION MODELS FOR COMPATIBILITY STUDIES REGARDING WRC-19 AGENDA ITEM 1.16.

²⁸ 6 GHz Report and Order.

- “[F]or separation distances of 30 meters or less, the free space pathloss model is the appropriate model.”²⁹
- “Beyond 30 meters and up to one kilometer from an unlicensed device to a microwave receiver, we find that the most appropriate propagation model is the Wireless World Initiative New Radio phase II (WINNER II).”³⁰
- “For separation distances greater than one kilometer . . . the Irregular Terrain Model combined with a clutter model depending on the environment is the most appropriate model.”³¹

These models are summarized in Table 4-1 below:

Table 4-1 - Summary of Propagation Model

Distance (Slant Range) from RLAN to Victim Receiver	Propagation Model
Up to 30 meters	Free Space Path Loss (FSPL)
30 meters to 1 km	<i>Combined LOS/NLOS Winner II</i> <ul style="list-style-type: none"> • Urban VLP: Winner II Scenario C2 • Suburban VLP: Winner II Scenario C1 • Rural VLP: Winner II Scenario D1
Above 1 km	<i>ITM + Clutter model</i> Clutter model <ul style="list-style-type: none"> • Urban/Suburban VLP: ITU-R Rec. P.2108-0 (Section 3.2.2) • Rural VLP: ITU-R Rec. P.452 Village Center Clutter

The combined median path loss model is computed using Eqn. 4-1 for distances between 30 m and 1 Km.

$$PL_{CWII} (\text{dB}) = PL_{LOS} (\text{dB}) \times Prob_{LOS} + PL_{NLOS} (\text{dB}) \times \{1-Prob_{LOS}\} \quad (4-1)$$

where,

- PL_{LOS} and PL_{NLOS} are the Line-of-Sight (LOS) and NLOS Path Losses per Table 4-4 in WINNER II Report³²
- $Prob_{LOS}$ is the LOS Probability per Table 4-7 in WINNER II Report

²⁹ *Id.* ¶ 64.

³⁰ *See id.* ¶ 66 (referencing the urban, suburban, and rural WINNER II channel models as C2, C1, and D1, respectively). *See also* WINNER & Information Society Technologies, *WINNER II Channel Models Part 1*, Table 2-1 Propagation scenarios specified in WINNER and Table 4-4 Summary table of the path-loss models, <https://www.cept.org/files/8339/winner2%20-%20final%20report.pdf> (“WINNER II Channel Models”).

³¹ *See 6 GHz Report and Order* ¶ 68 (referencing the *Irregular Terrain Model Guide*). *See also* G.A. Hufford et al., *A Guide to the Use of the ITS Irregular Terrain Model in the Area Prediction Mode*, NTIA Report 82-100 (1982), https://www.ntia.doc.gov/files/ntia/publications/ntia_82-100_20121129145031_555510.pdf.

³² *See* WINNER II Channel Models.

In addition to the combined median path loss term, the Winner II LOS and NLOS Path Loss components include a random lognormal shadowing term that is included in the simulations.

For distances above 1 km, ITM with the SRTM 3-arc-seconds Terrain Database is used. The P.452 village center clutter loss of 18.4 dB is used for the 1.5m RLAN device when the following conditions are met:

- RLAN elevation angle towards the victim receiver ≤ 2.86 deg (corresponding to a VLP deployed at an average distance from a village building of average height), AND
RLAN distance to victim receiver ≥ 0.7 km

4.3 RLAN to Terrestrial MSS Gateway Models

Possible interference paths from RLANs to the earth stations antenna at the future MSS gateway site are similar to those described in Section 4.2 for paths from terrestrial systems to terrestrial FS systems, which includes a terrain model. Like Sections 4.1 and 4.2, paths from indoor RLANs to MSS gateway antenna experience penetration loss calculated using P.2109 as the path exits a building.

The MSS downlink signal from the selected MSS satellite at the randomly selected moment in time received at the MSS gateway's earth station is line-of-site and thus the free space path loss model was used.

5 Sharing Results

5.1 FSS Uplink Sharing

This section reports the results of an aggregate I/N calculation into a number of satellite uplink beams using the RLAN deployment per Section 3.1.1 and available satellite G/T contours³³, related to the satellites in Table 5-1. A search of the ITU BR IFIC database provided information on the 52 satellites that Mexico brought to use in the 6 GHz band. For purposes of providing a conservative analysis, satellite beams with higher G/T over Mexico or bigger coverage of areas have been chosen. Peak G/T levels per the satellites' filings are used to derive the absolute G/T levels from the G/T contours (that indicate amount of dB down from peak G/T). In addition to the three Satelites Mexicanos, S.A. DE C.V. satellites (Satmex 6, Satemex, and Satmex 8), three other satellites were selected based on their maximum G/T value over Mexico. Consequently, no effort was made to establish whether any of the three latter satellites selected are currently in use over Mexico. For example, the satellite could have provided coverage over Mexico when launched, but it may have been relocated subsequently to provide coverage to a different geography. In another instance, the satellite could have been in operation for years, but no longer. If the risk of harmful interference from 6 GHz RLAN operations to the satellite-based fixed service uplinks for each of these six satellites is negligible, then the presumption is that risk of harmful interference to other satellites providing service across Mexico is even less.

³³ Extracted from ITU BR IFIC

The analysis has been applied to a satellite channel plan assuming 36 MHz channels in 40 MHz occupied bandwidth on two polarizations. Each channel on each satellite has been subject to 10 independent RLAN deployments of a Monte Carlo simulation as detailed in the next Section. Table 5-1 gives the worst I/N value found for each beam across all channels. The table shows that, in all cases, the I/N is lower than absolute value of -26.92 dB.

Table 5-1 - Summary worst-case I/N into FSS

Satellite Longitude	Satellite Name	Beam Reference	Populations included in calculation	Worst aggregate I/N (dB)
116.8° West	Satmex 8	cuh.gxt	Mexico, all of the Americas and the Caribbean	-30.15
114.9° West	Eutelsat 115 West B (Satmex 7)	crhco.gxt	Mexico, all of the Americas and the Caribbean	-27.08
113° West	Satmex 6	chuh.gxt	Mexico, all of the Americas and the Caribbean	-31.01
103° West	SES-3	crv.gxt	Mexico, all of the Americas and the Caribbean	-31.34
97° West	Galaxy 19	crf_c.gxt	Mexico, all of the Americas and the Caribbean	-29.73
47.5° West	NSS-806	hau.gxt	Mexico, all of the Americas and the Caribbean, Europe, Africa	-26.92

5.1.1 FSS Simulation Methodology

Interference from RLAN deployments into FSS satellite receiver is simulated using a Monte Carlo simulation of the RLAN deployment generated from the various probability distributions given in Section 3.

The basic structure of the simulation is as follows:

1. Data setup:
 - a. Define the simulation region and create a database of population density at points within the simulation region;
 - b. Transform population data over the simulation region to active RLAN device population probability distribution over the simulation region;
 - c. Specify the orbital slot of the FSS satellite receiver and the G/T values over the simulation region;
 - d. Specify a list of FSS satellite channels to simulate.
2. Monte-Carlo iterations:

- a. Generate a random layout of RLANs using the device population probability distribution;
 - b. Generate a random transmit EIRP, height, body loss, RLAN channel, clutter loss and building entry loss values between each RLAN and FSS satellite receiver in accordance with the RLAN distributions in Section 3.2 and propagation modelling set out in Section 4;
 - c. Compute the aggregate interference from all co-channel RLANs into the FSS satellite receiver for each of the simulated FSS channels.
3. Iterate:
 - a. Repeat Step 2 for the total specified number of iterations;
 - b. Record I/N values for each FSS channel on each iteration and write results to a file.
 4. Average the recorded aggregate I/N values (over the performed iterations) to create plot of average I/N versus FSS channel number.

Steps 1 and 2 above are further elaborated below.

Step 1: Data Setup

A population matrix file is created. Each row/line of the matrix contains a Longitude (LON)/Latitude (LAT) coordinate and the population density at that location. Furthermore, there is a region ID that specifies if the point is in Europe, Africa, Mexico or the Americas but not in Mexico. The matrix resolution is 30 arcseconds for both LON and LAT coordinates.

Note that the collection of all points in the population density file defines the simulation region and the simulation region is, in general, not rectangular. Grid points that are in the ocean or other locations that are not part of the simulation are omitted from the population density file. Each grid point is classified as being URBAN, SUBURBAN or RURAL depending on the population density value for the grid point and threshold values that are inputs to the simulation.

The population density file is used to produce the active RLAN device population probability distribution over the simulation region. The first step is to convert population density values into population values for each grid point by multiplying the population density by the area of the 30 arcsec x 30 arcsec region centered at the grid point. These population values are then summed for each of the regions Europe, Africa, Mexico and Americas³⁴ but not in Mexico.

Let PE, PA, PM and PN be the populations of Europe, Africa, Mexico and the Americas but not in Mexico respectively. Let NE, NA, NM, NN be the number of active RLAN devices in each region respectively. These values are inputs to the simulation.

For each grid point, the population value is converted to the average active RLAN device count by multiplying by (NE/PE), (NA/PA), (NM/PM) or (NN/PN) depending on whether the grid point is in Europe, Africa, Mexico, or the Americas but not in Mexico. This is then converted into a large discrete probability distribution function where each grid point is assigned a probability equal to the average RLAN device count at that grid point divided by the total active RLAN device count. A random RLAN position is generated by generating a random grid point using this discrete probability distribution, then

³⁴ Americas refers to Central America, North America, South America and the Caribbean.

selecting a location uniformly distributed over the 30 arcsec x 30 arcsec region centered at the grid point.

The values of G/T over the simulation region are specified in the GXT format. This standard file format specifies contours over which G/T values are constant. Given an arbitrary LON/LAT position, two contours are identified for which this position is between and the G/T value is taken to be the average of the corresponding G/T values. Furthermore, the region outside the outermost contour, when less than or equal to 20 dB below the peak, is set to that contour. When the outermost contour is greater than 20 dB below peak (e.g., 10 dB below peak), the region is set 20 dB below peak in the absence of the beam roll-off pattern.

The list of FSS channels to be simulated is specified by a channel bandwidth, center-to-center channel spacing, start center frequency and number of channels simulated. Figure 5-1 shows the nominal FSS transponder plan between 5925 to 6425 MHz that has been assumed. Each transponder has a bandwidth of 36 MHz and is spaced 40 MHz apart. Over this 500 MHz band there are 24 transponders, 12 in each polarization. The channel center frequencies for each polarization are staggered by 20 MHz. The start frequency is 5927 MHz.

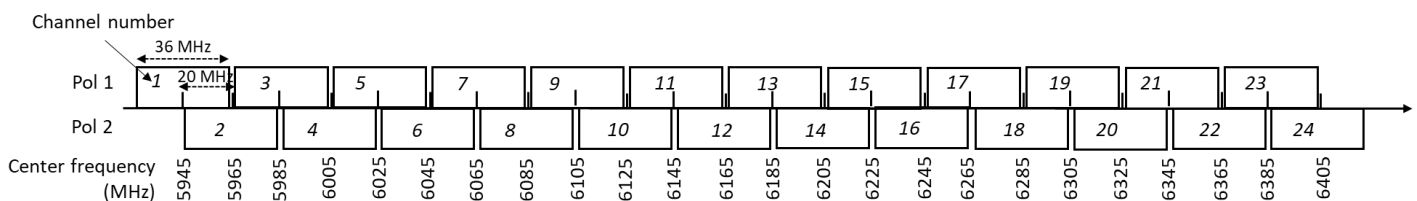


Figure 5-1 - Representative FSS Transponder Frequency Plan (f_c , Separation=40MHz per polarization (Pol))

Step 2: Monte Carlo Iterations

For each iteration, a random layout of active RLAN devices is generated one RLAN at a time. Each RLAN device is assigned a random longitude/latitude position generated using the device population probability distribution described above. Each RLAN device is assigned a random height, EIRP, body loss, and building type using discrete probability distributions according to Section 3.2. Building types are outdoor (meaning no building attenuation) RLAN, indoor-traditional or thermally efficient (respecting a 20% thermally efficient/ 80% traditional balance). Each RLAN is assigned a random bandwidth using a discrete probability distribution as in Table 3-9 and a random center frequency as in Figure 3-9. The center frequency is generated by considering all possible center frequencies for the selected bandwidth and using a uniform distribution.

For each RLAN, a 4/3 earth model is used to determine whether the satellite is in view or over the horizon. RLANS for which the satellite is not in view are considered to contribute no interference to the satellite and are thus ignored in the interference calculation.

For each FSS channel in the simulation, interference from all RLANS for which the satellite is in view is computed and aggregated. The RLAN bandwidth and center frequency along with the FSS channel bandwidth and center frequency are used to compute the fraction of the WAS/RLAN bandwidth that overlaps with the FSS channel. If there is no overlap, the RLAN contributes no interference to the FSS

channel. In addition, a random body loss is generated using discrete probability distributions described in Sections 3.2.2 and 3.2.3.

A random building entry loss is computed using Recommendation ITU-R P.2109-0 using the building type and elevation angle from the RLAN to the FSS satellite receiver orbital slot. Note that for outdoor RLANs the building entry loss is 0 dB. Random path clutter values are generated per Recommendation ITU-R P.2108 for urban and suburban RLANs and per Recommendation ITU-R P.452 for rural RLANs (as described in Section 4).

The path loss is computed using Free Space Path Loss (FSPL), per Recommendation ITU-R P.619-3, from the RLAN position to the FSS satellite orbital slot. Polarization loss of 3 dB is added. The FSS satellite Figure-of-Merit (G/T) is computed at the RLAN position as described above. The I/N contribution for a single RLAN into an FSS channel is computed by:

$$\frac{I}{N} = EIRP + G_{FarField} - L_{Body} - L_{Bldg} - FSPL - L_{Clutter} - L_{Polarization} - L_{SpectralOverlap} + \frac{G}{T} - 10\log_{10}(kB)$$

Where,

- $EIRP$ (dBW) = RLAN EIRP (Table 3-4 as modified by Table 3-7 and Table 3-8) for LPI and Standard Power; 14 dBm for VLP) within RLAN channel bandwidth (Table 3-9)
- $G_{FarField}$ (dB) = VLP far field gain that includes body loss (see Section 3.2.3); 0 dB for LPI and Standard Power RLANs
- L_{Body} (dB) = LPI and Standard Power Body Loss (see Section **Error! Reference source not found.**); 0 dB for LPI
- L_{Bldg} (dB) = Building Entry Loss
- $FSPL$ (dB) = $92.45 + 20*\log_{10}(\text{RLAN center frequency in GHz}) + 20*\log_{10}(\text{RLAN distance to FS Rx in Km})$
- $L_{Clutter}$ (dB) = Clutter Loss
- $L_{Polarization}$ (dB) = Polarization Loss of 3 dB
- $L_{SpectralOverlap}$ (dB) = $10*\log_{10}(\text{spectrum overlap between RLAN channel and victim channel / RLAN bandwidth})$, also called frequency-dependent rejection
- $\frac{G}{T}$ (dB/K) = Satellite receiver Figure-of-Merit (dB/K)
- k (J/K) = Boltzmann's constant = $1.3806488 \times 10^{-23}$
- B (Hz) = FSS channel bandwidth (Hz)

This I/N is aggregated over all RLANs for each FSS channel in the simulation.

5.1.2 RLAN Populations used in the Simulations

The following total population projections for 2025, for each region, have been used in generating RLAN deployments in the simulations.

1. Mexico, Total population: 141,132,000
2. The Americas (except Mexico) and the Caribbean, Total population: 934,760,659

3. Europe (48 CEPT states), Total Population: 768,589,000³⁵
4. Africa, Total Population: 1,407,870,000³⁶

Using the total populations per above and same³⁷ assumptions as Table 3-1, Table 5-2 shows number of simultaneously transmitting RLAN devices that are simulated in each region within the satellite footprint. In addition, the number of active RLANs in Africa is divided by factor of 4³⁸ to reflect the delay in maturity of RLANs deployment at 6 GHz.

Table 5-2 – Number of active RLAN devices simulated

Region	2025 Population	Number of instantaneously transmitting RLAN devices
Mexico	141,132,000	179,261
The Americas (except Mexico) and the Caribbean	934,760,659	1,194,849
Europe	768,589,000	988,040
Africa	1,407,870,000	458,132

5.1.3 Results by FSS Satellite Beam

5.1.3.1 Satmex 8 (116.8° W)

The Satmex-8 satellite at 116.8° west has a hemispheric beam with a peak G/T of 1.3 dB/K. The G/T contours are shown below.

³⁵ CEPT ECC, *Report 302: Sharing and Compatibility Studies Related to Wireless Access Systems Including Radio Local Area Networks (WAS/RLAN) in the Frequency Band 5925-6425 MHz* (May 29, 2019),

<https://docdb.cept.org/download/cc03c766-35f8/ECC%20Report%20302.pdf> (“ECC Report 302”). Page 86.

³⁶ *Id.*

³⁷ Except for the percentage of population in Urban/Suburban/Rural that were derived for each region using the population density thresholds in Section 3.1.2.

³⁸ ECC Report 302, Page 87.

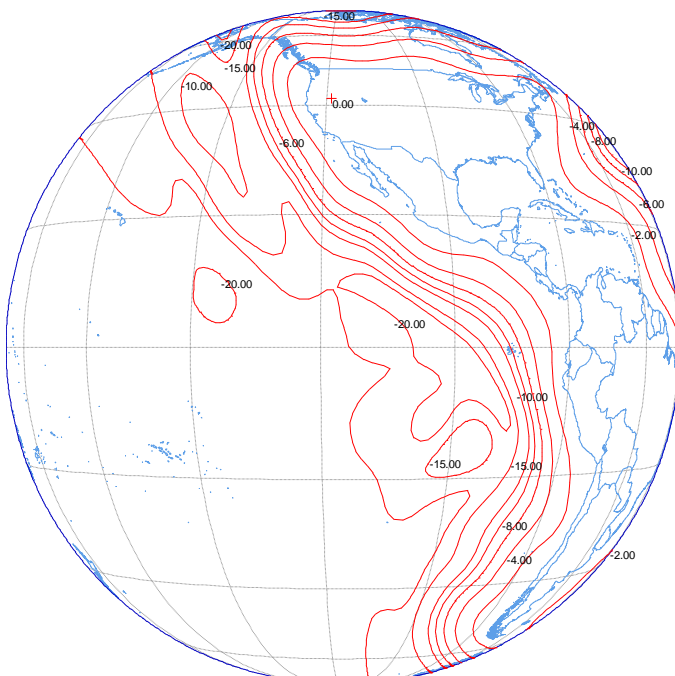


Figure 5-2: Satmex-8 G/T Contours (cuh.gxt)

The aggregate I/N across the 24 modelled FSS channels, averaged over 10 simulation iterations is shown in the figure below. The calculation includes RLANs in Mexico, Central America, North America, South America and the Caribbean.

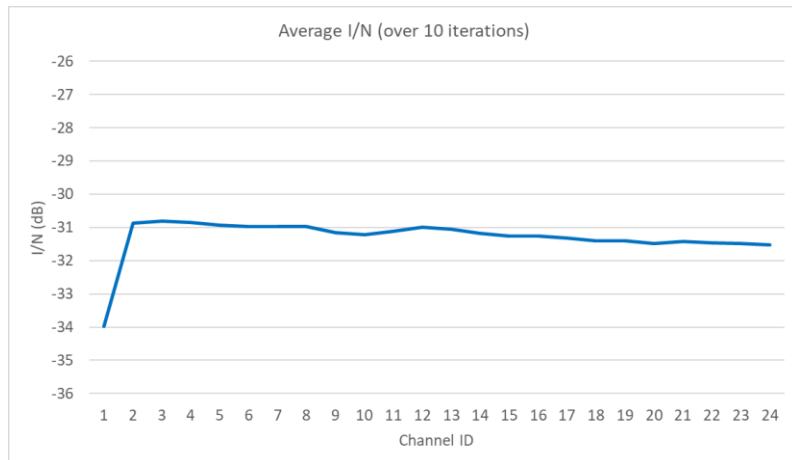


Figure 5-3: Satmex-8 I/N per channel

The maximum I/N found in a single iteration is -30.15 dB. The maximum averaged over 10 iterations is -30.82 dB.

5.1.3.2 Eutelsat 115 West-B (Satmex 7) (114.9° W)

The Eutelsat 115 West-B satellite at 114.9° west has a hemispheric beam with a peak G/T of 5.8 dB/K. The G/T contours are shown below.

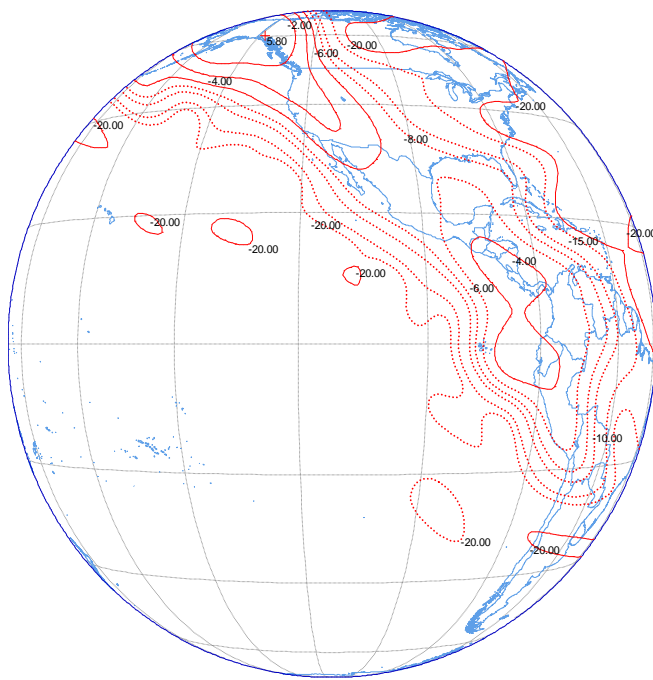


Figure 5-4: Eutelsat 115 West-B G/T Contours (crhco.gxt)

The aggregate I/N across the 24 modelled FSS channels, averaged over 10 simulation iterations is shown in the figure below. The calculation includes RLANs in Mexico, Central America, North America, South America and the Caribbean.

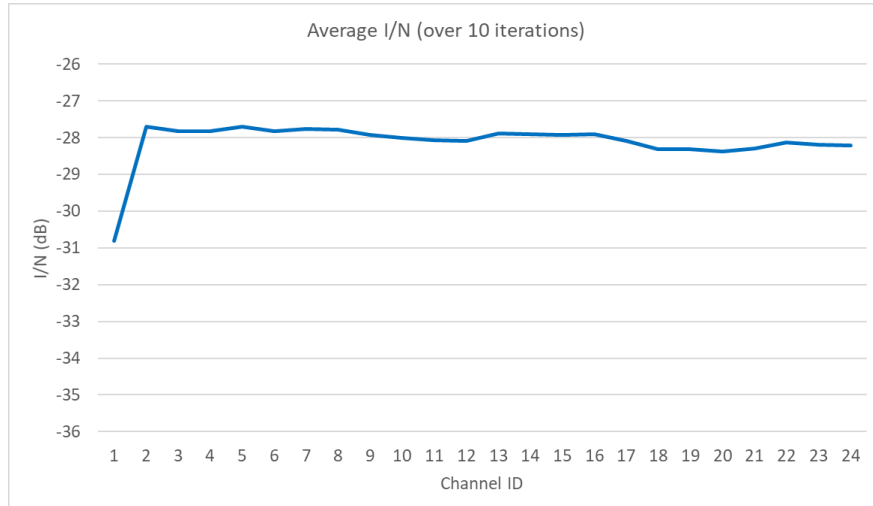


Figure 5-5: Eutelsat 115 West-B I/N per channel

The maximum I/N found in a single iteration is -27.08 dB. The maximum averaged over 10 iterations is -27.70 dB.

5.1.3.3 Satmex 6 (113° W)

The Satmex-6 satellite at 113° west has a hemispheric beam with a peak G/T of 1.7 dB/K. The G/T contours are shown below.

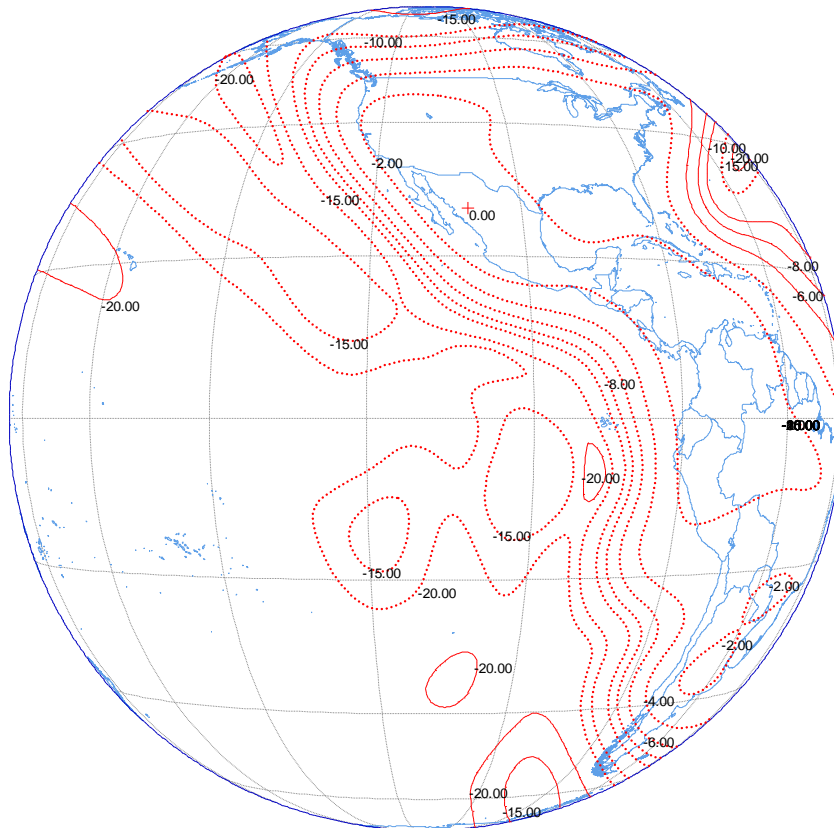


Figure 5-6: Satmex-6 G/T Contours (chuh.gxt)

The aggregate I/N across the 24 modelled FSS channels, averaged over 10 simulation iterations is shown in the figure below. The calculation includes RLANs in Mexico, Central America, North America, South America and the Caribbean.

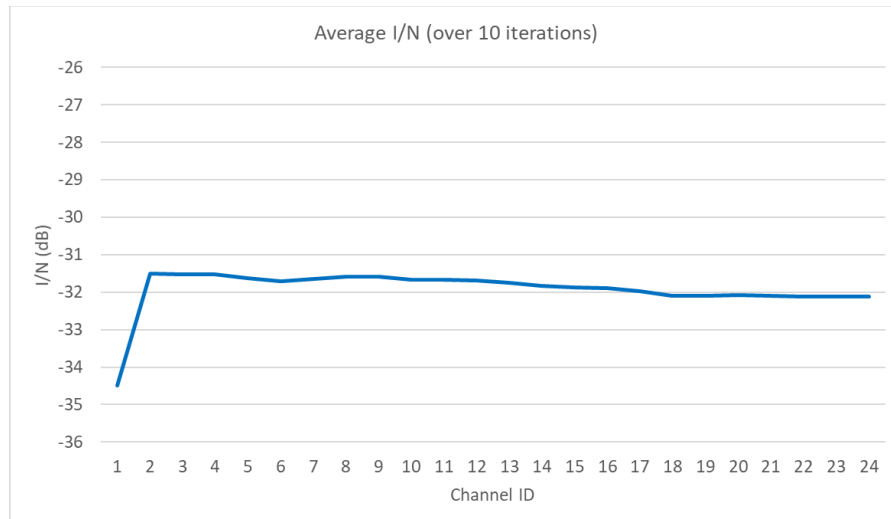


Figure 5-7: Satmex-6 I/N per channel

The maximum I/N found in a single iteration is -31.01 dB. The maximum averaged over 10 iterations is -31.50 dB.

5.1.3.4 SES-3 (103° W)

The SES-3 satellite at 103° west has a spot beam with a peak G/T of 5.3 dB/K. The G/T contours are shown below.

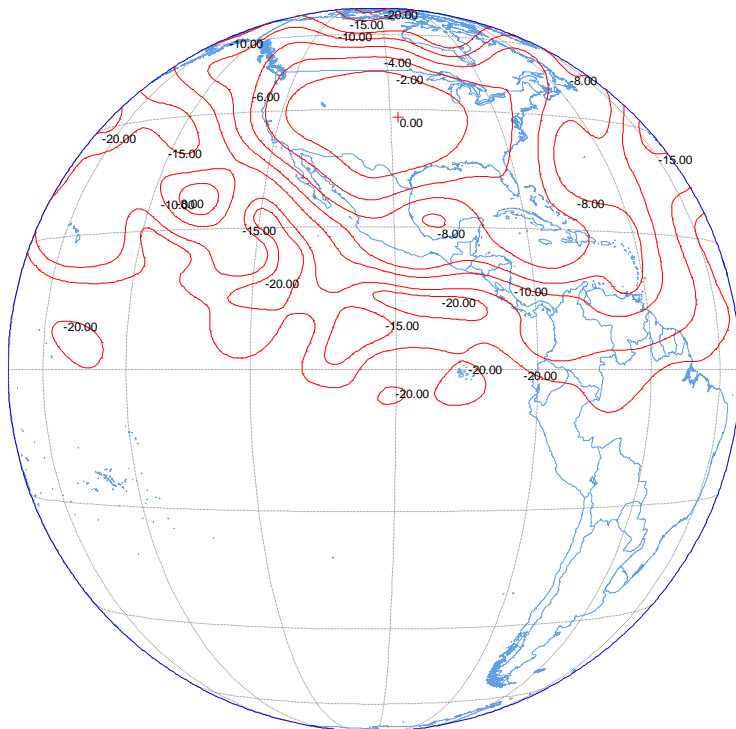


Figure 5-8:SES-3 G/T Contours (crv.gxt)

The aggregate I/N across the 24 modelled FSS channels, averaged over 10 simulation iterations is shown in the figure below. The calculation includes RLANs in Mexico, Central America, North America, South America, and the Caribbean.

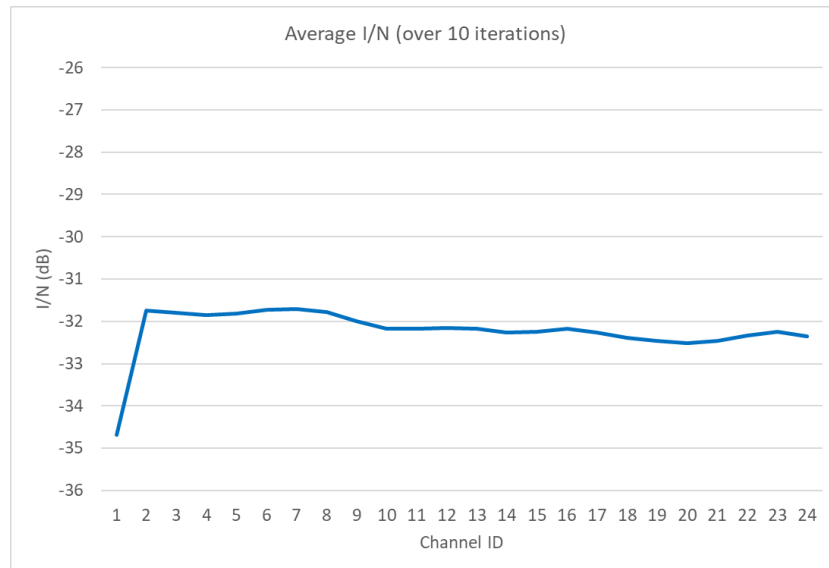


Figure 5-9: SES-3 I/N per channel

The maximum I/N found in a single iteration is -31.34 dB. The maximum averaged over 10 iterations is -31.71 dB.

5.1.3.5 Galaxy-19 (97° W)

The Galaxy-19 satellite at 97° west has a spot beam with a peak G/T of 4.6 dB/K. The G/T contours are shown below.

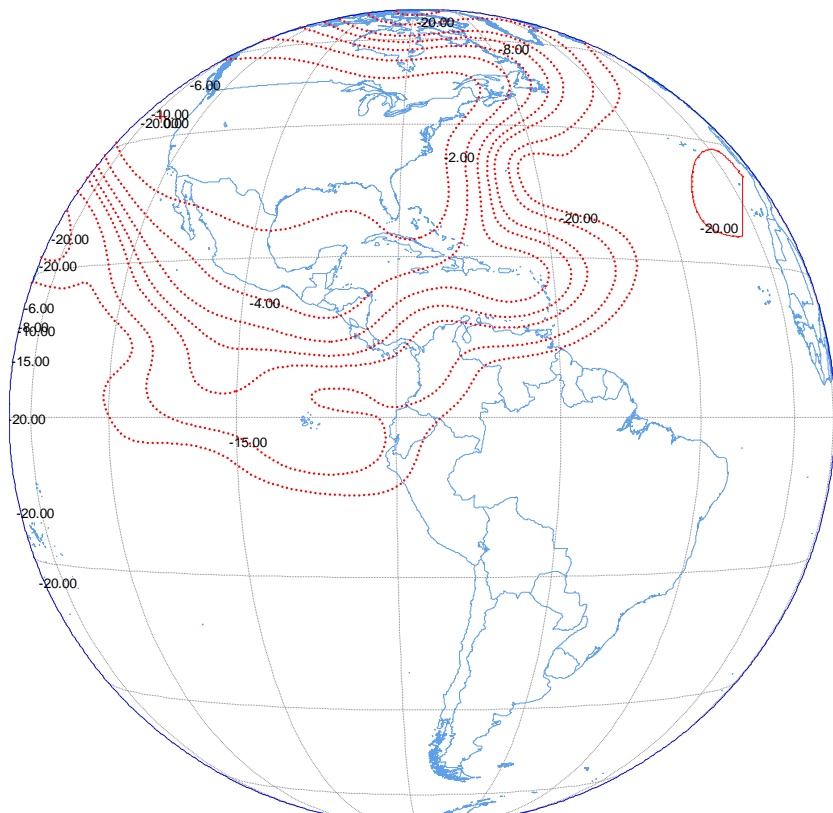


Figure 5-10: Galaxy-19 G/T Contours (crf_c.gxt)

The aggregate I/N across the 24 modelled FSS channels, averaged over 10 simulation iterations is shown in the figure below. The calculation includes RLANs in Mexico, Central America, North America, South America, and the Caribbean.

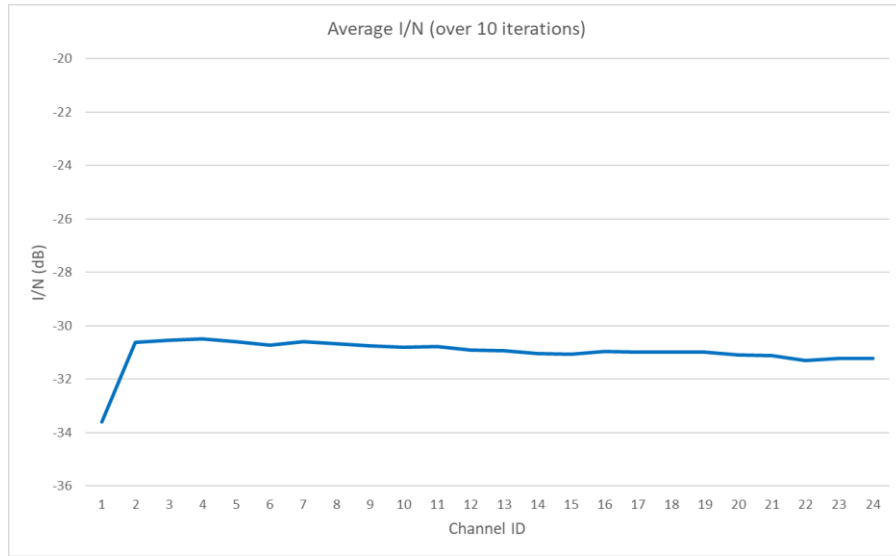


Figure 5-11: Galaxy-19 I/N per channel

The maximum I/N found in a single iteration is -29.73 dB. The maximum averaged over 10 iterations is -30.50 dB.

5.1.3.6 NSS-806 (47.5° W)

The NSS-806 satellite at 47.5° west has a hemispheric beam and a regional beam with a peak G/T of 3.1 dB/K. The G/T contours are shown below.

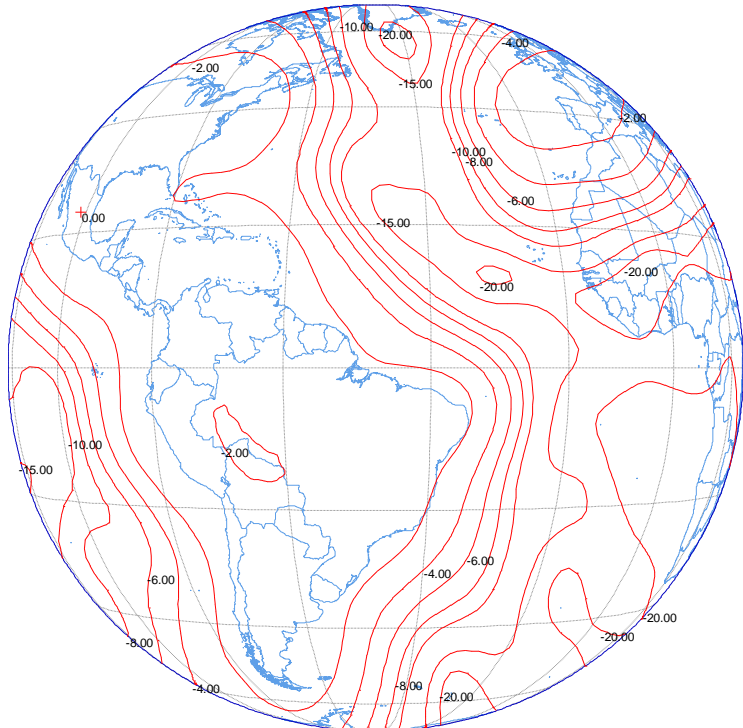


Figure 5-12: NSS-806 G/T Contours (hau.gxt)

The aggregate I/N across the 24 modelled FSS channels, averaged over 10 simulation iterations is shown in the figure below. The calculation includes RLANs in Mexico, Central America, North America, South America, the Caribbean, Europe and Africa.

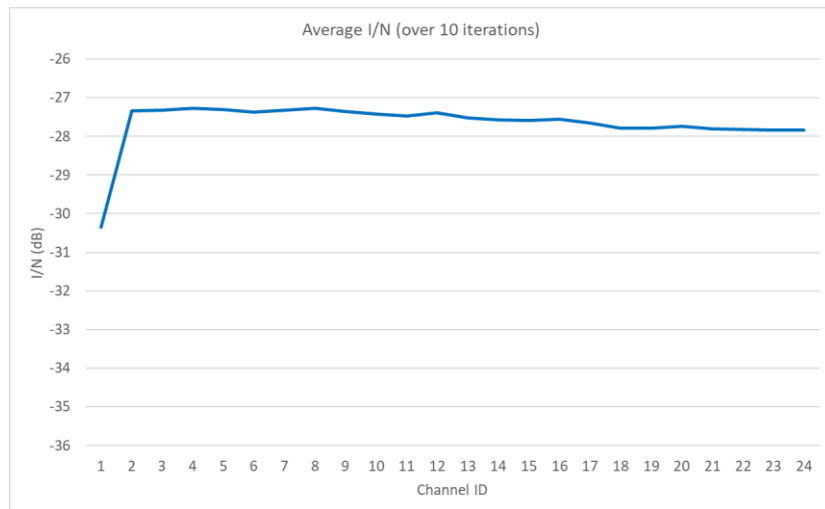


Figure 5-13: NSS-806 I/N per channel

The maximum I/N found in a single iteration is -26.92 dB. The maximum averaged over 10 iterations is -27.27 dB.

5.1.4 FSS Link Budgets

Table 5-3 shows aggregate link budget for Satmex 7 (Eutelsat 115 West-B) which has the highest peak G/T and the highest I/N levels after NSS-806.

As indicated in this table, the average Building Entry Loss, Clutter Loss, Free Space Path Loss and G/Ts are the averages over the values used by the Monte Carlo simulation amongst all the RLANs within the corresponding region. Averaging for the transmit powers and simulation parameters (building entry losses, clutter losses and G/T values) are done in linear domain. Note that this results in much lower building entry and clutter losses than their mean values, i.e. 50th percentile.

The link budgets match the Monte Carlo simulation results within about 3 dB for this satellite. The differences are due to the coarse approximation of the link budget versus the very detailed precise calculations in the Monte Carlo simulation.

Table 5-3 - Satmex 7 (at 114.9 West) link budget

Parameter	Unit	Mexico	The Americas (except Mexico) and the Caribbean	Source
Number of Active RLANs		179,261	1,194,849	Table 5-2
Number of Active RLANs contributing to I/N		179,162	604,121	RLANs within the coverage area
Total Average EIRP per RLAN	mW	69.80	69.80	Includes body loss for LPI and Standard Power Client devices per Section 3.2.2 and Average (in linear domain)

				far-field gain for VLP devices per Section 3.2.3
Average Building Entry Loss (Indoor RLAN)				
Traditional Building	dB	-17.91	-14.06	Simulation; Average in linear domain
Thermally Efficient Building	dB	-23.27	-21.44	
Total Aggregate Average EIRP (all RLANs)	dBW	27	34	Includes Building Loss
Bandwidth Correction		0.031	0.031	= Satellite Noise Bandwidth / Total RLAN Band (5945 to 7125 MHz)
Total Aggregate Average EIRP (bandwidth correction)	dBW	12	18	
Average Free Space Path Loss (FSPL)	dB	-199.97	-200.43	Simulation
Polarization Loss	dB	-3	-3	
Average Clutter Loss	dB	-0.62	-2.20	Simulation; Average in linear domain
Total Aggregate Interference Power at Satellite	dBW	-191.95	-187.16	
Satellite Receiver Antenna Peak G/T	dB/K	5.8	5.8	Not used;
Satellite Receiver Antenna Avg. G/T	dB/K	5.11	2.90	Simulation; Average in linear domain over the area
Boltzmann's Constant	dBW/K/Hz	-228.60	-228.60	
Satellite Noise Bandwidth	MHz	36.0	36.0	
Calculated Average I/N	dB	-33.80	-31.23	
Simulated Max I/N	dB	-34.12	-27.81	Simulation
“Calculated Average I/N” – “Simulated Max I/N”	dB	0.32	-3.42	

5.1.5 FSS Sharing Conclusions

Simulations show that in all cases studied, the I/N for all satellites in all channels is less than -26.92 dB. It can be concluded that RLANs in the three device classes operating over a 20, 40, 80, or 160 MHz channel bandwidth do not cause harmful interference to an FSS uplink in the 6 GHz band.

5.2 Fixed Service (FS) Sharing

This Section describes analyses performed to investigate the impact of RLAN interference on FS links.

A detailed Monte-Carlo simulation of the interference environment was performed for the FS in Mexico City for which the data was available. The accuracy of this data was not validated to confirm whether they represent real FS link. However, the data could represent potential FS links in this region.

The Monte-Carlo simulations were performed over a large number of independent events to establish long-term statistical properties in the environment.

5.2.1 FS Data

27 FS links in the vicinity of Mexico City were used in the simulation. Figure 5-14 to Figure 5-19 show the cumulative distribution function (CDF) of the FS characteristics that were used in the simulation, which were: FS Bandwidth, FS Rx peak Gain, FS Rx feederloss, FS Rx height above ground level, FS Rx AMSL³⁹ (Above Mean Sea Level) Height – FS Tx AMSL Height, and FS link

³⁹ Note that the simulation uses SRTM terrain height while Figure 5-18 shows AMSL height (height above ground level + terrain height) using terrain height in the FS data.

distance. These figures show the range of values as well as the median (50^{th} percentile) values used. As indicated, this data can represent real FS links.

In addition to these parameters, the other parameters that were used from the FS data in the simulation were the FS Tx and Rx latitude and longitude, and FS center frequency. Figure 5-20 shows the location of the 27 FS Tx-Rx links in Google Earth. The numbers correspond to the 27 unique FS ID's.

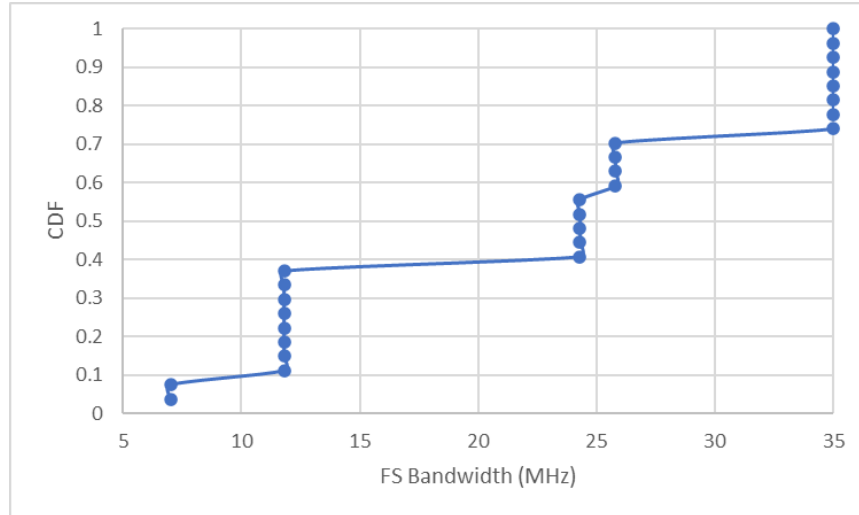


Figure 5-14 - CDF of FS Bandwidth for 27 FS simulated in vicinity of Mexico City

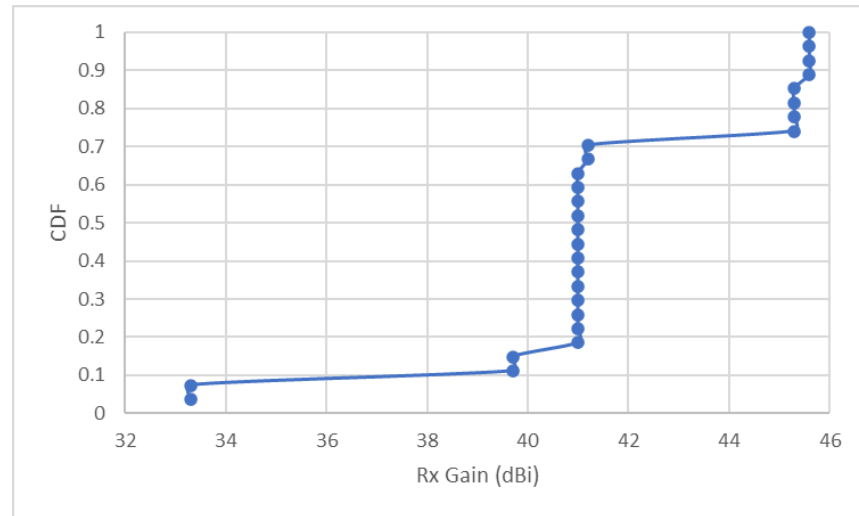


Figure 5-15 – CDF of FS Rx peak Gain for 27 FS simulated in vicinity of Mexico City

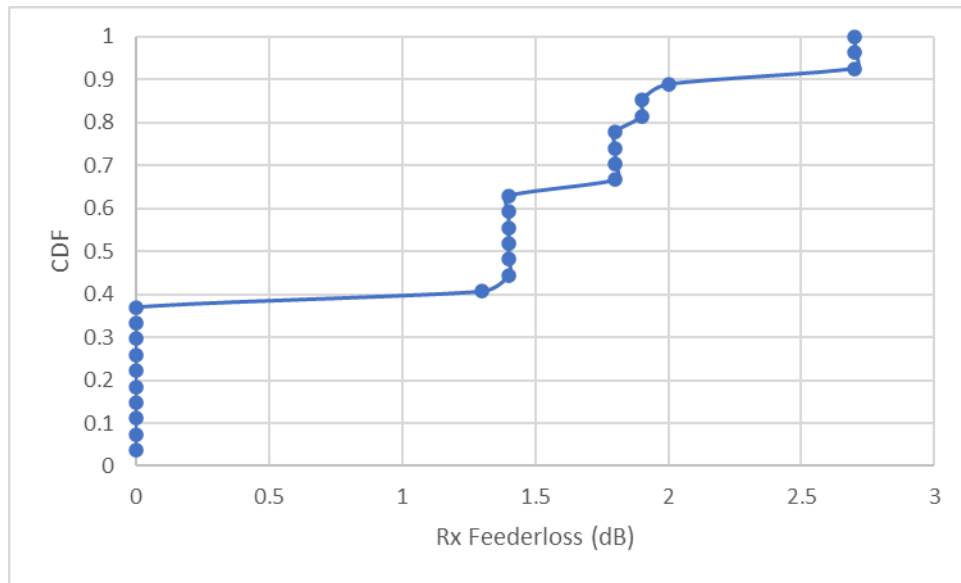


Figure 5-16 - CDF of FS Rx Feederloss for 27 FS simulated in vicinity of Mexico City

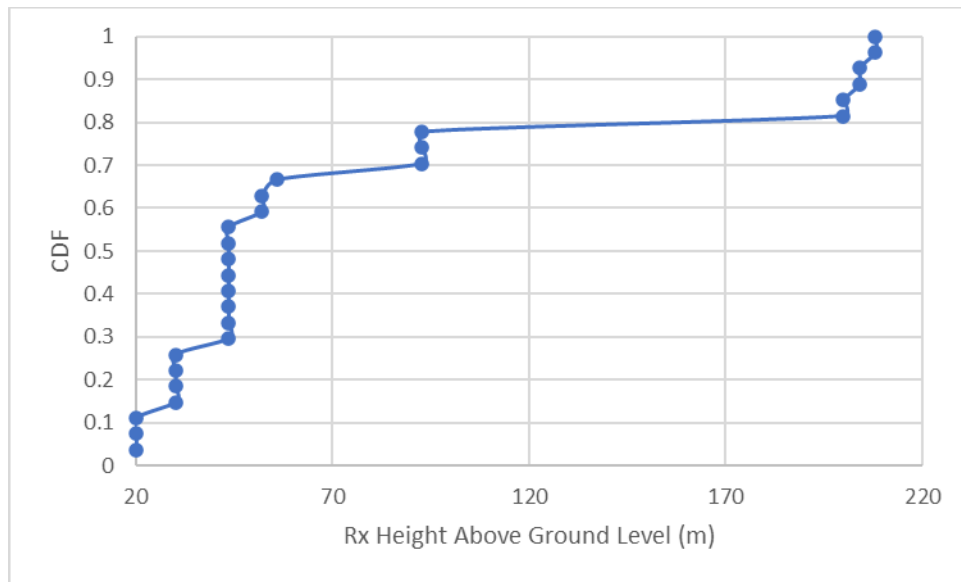


Figure 5-17 - CDF of FS Rx Height Above-Ground-Level for 27 FS simulated in vicinity of Mexico City

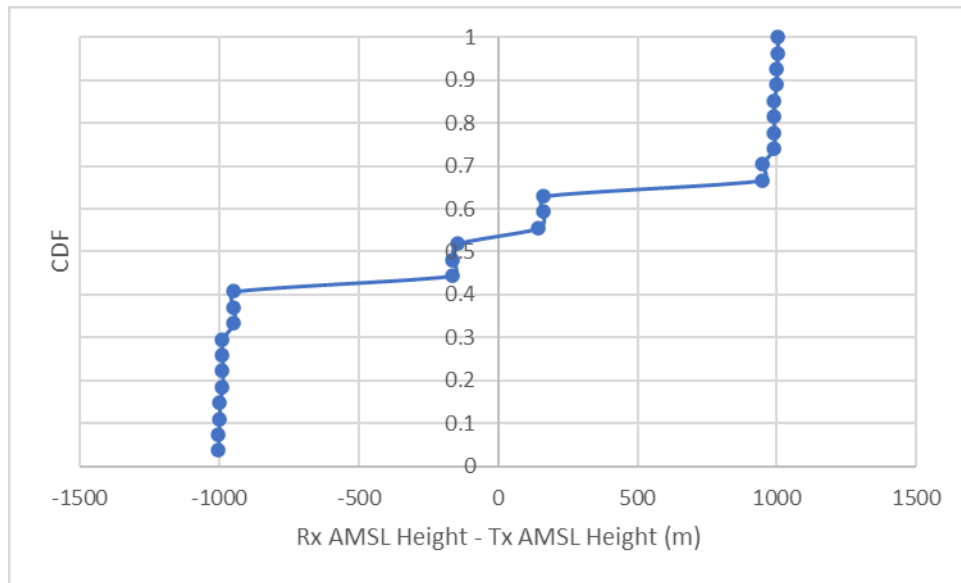


Figure 5-18 - CDF of $(Rx\ Aerial\ Mean\ Sea\ Level\ Height - Tx\ Aerial\ Mean\ Sea\ Level\ Height)$ for 27 FS simulated in vicinity of Mexico City

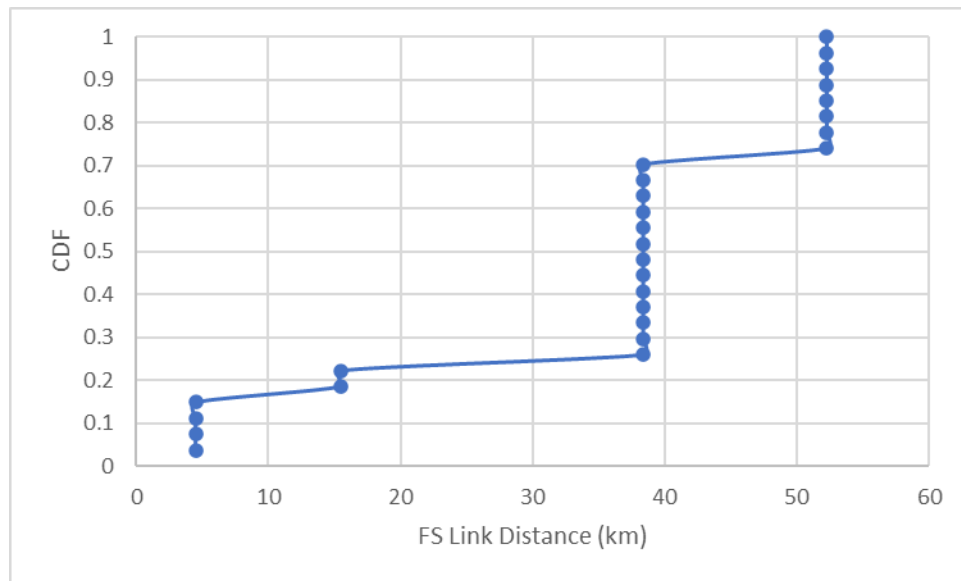


Figure 5-19 – CDF of FS link distance



Figure 5-20 – Location of 27 simulated FS links (yellow markers at FS Tx and FS Rx and white 3dB beamcone from FS Rx to FS Tx)

5.2.2 Key Modeling Assumptions

5.2.2.1 RLAN Device Deployment

As described in Section 3.1.1, the RLANs were randomly distributed throughout Mexico based on population density. The drop process is detailed in Step 2 of Section 5.1.1.

5.2.2.2 FS Receiver Antenna Performance

ITU-R Recommendation F.1245⁴⁰ was used to model the FS antenna sidelobe performance. As shown in Figure 5-21, commercial antennas (such as UHX10 that is used by some of Mexico's FS), portrayed by the red line in the figure, significantly outperform F.1245. By using F.1245 this analysis overstates the interference and provides very conservative results.

⁴⁰ International Telecommunication Union, *F.1245: Mathematical Model of Average and Related Radiation Patterns for Point-to-Point Fixed Wireless System Antennas for Use in Interference Assessment in the Frequency Range From 1 GHz to 86 GHz*, Recommendation F.1245 (2019), available at <https://www.itu.int/rec/R-REC-F.1245/en>.

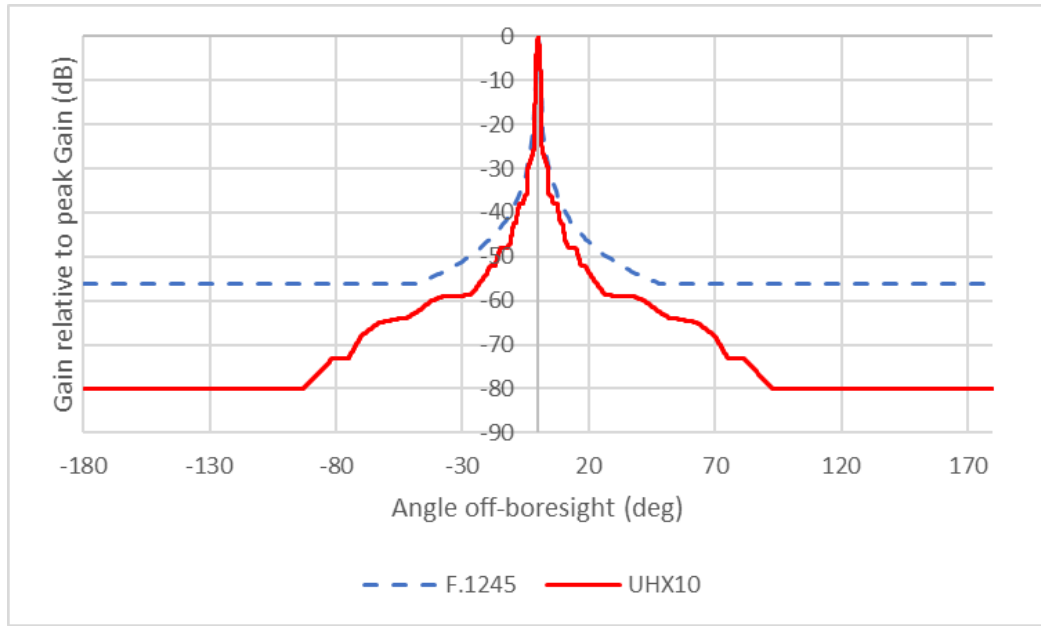


Figure 5-21 - Comparison of ITU-R 1245 and Ultra-High-Performance Antenna (UHX10) Radiation Patterns

5.2.2.3 FS Simulation Methodology

Monte-Carlo simulations were performed to calculate RLAN interference to each of the 27 FS stations in the vicinity of Mexico City. For each iteration, active RLANs were randomly placed, with their locations weighted according to the population density. The aggregate interference power to each of the FS stations were then calculated. One hundred thousand simulation iterations were then performed to gather statistics on the interference.

The interference power, I , is computed per Eqn. 5-2 below:

$$I = EIRP + G_{FarField} - L_{body} - L_{Bldg} - L_{PropagationPath} - L_{SpectralOverlap} - L_{Polarization} - L_{feed} + G_{Rx-to-RLAN} \quad (5-2)$$

where,

- I (dBW) = Interference Power from an RLAN device
- $EIRP$ (dBW) = RLAN EIRP (Table 3-4 as weighted by Tables 3-7 and 3-8) for LPI and Standard Power; 14 dBm for VLP) within RLAN channel bandwidth (Table 3-9)
- $G_{FarField}$ (dB) = VLP far field gain that includes body loss (see Section 3.2.3); 0 dB for LPI and Standard Power RLANs
- L_{body} (dB) = LPI and Standard Power RLAN Body Loss (see Section 3.2.2); 0 dB for VLP
- L_{Bldg} (dB) = Building Entry Loss
- $L_{PropagationPath}$ (dB) = Propagation Path loss including Clutter loss (Section 4.1)

- $L_{SpectralOverlap}$ (dB) = $10 \log_{10}(\text{spectrum overlap between VLP channel and victim channel / VLP bandwidth})$, also called frequency-dependent rejection.
- $L_{polarization}$ = Polarization Loss of 3 dB^{41,42}
- L_{feed} (dB) = Feederloss of victim FS receiver (per FS data)
- $G_{Rx-to-RLAN}$ (dBi) = Gain of victim FS Rx towards RLAN based on the angle off-boresight

The I/N is the ratio of the interference power and the receiver (Rx) noise power. The receiver noise power is calculated, for each victim Rx, using Eqn. 5-3 below:

$$N = 10(kT_0B) + NF \text{ (dBW)} \quad (5-3)$$

where,

- N = Victim FS Rx noise power at receiver input (dBW)
- k = Boltzmann's constant = $1.38064852 \times 10^{-23} \text{ m}^2 \text{ kg s}^{-2} \text{ K}^{-1}$
- T_0 = 290 K
- B = Victim Rx Bandwidth (Hz)
- NF = Victim FS Rx Noise Figure (dB) = 4 dB (per FS data)

Note that Noise Figure of 4 dB is conservative. For example, in the co-existence studies conducted by the EU 5dB Rx Noise Figures was considered.

For each FS in the simulation, this I/N is aggregated over all RLANs.

Next, for these FS stations, the resulting increase in FS unavailability was calculated and analyzed.

5.2.3 Aggregate Interference Simulation

One hundred thousand simulation iterations were performed to determine the aggregate I/N at each of 27 FS receive locations. Together these simulations represent 2,700,000 different RLAN-to-FS interference morphologies with more than 17.92 billion total number of active RLANs dropped in Mexico City, which represent an excellent statistical model of expected interference. The occurrence probability for aggregate I/N > -6 and 0 dB was computed. To ensure inclusion of every RLAN that could affect a receiver, while avoiding the unnecessary complexity of modeling every RLAN in

⁴¹ International Telecommunication Union, *Working Document Towards a Preliminary Draft New Report ITU-R M.[RLAN SHARING 5150-5250 MHZ] - Sharing and Compatibility Studies of WAS/RLAN in the 5 150-5 250 MHz Frequency Range*, Appendix 2, Section 5.1.6.7 (Nov. 2017) (noting that with regard to polarization mismatch, a value of 3 dB is considered according to what has been supported by France during TG-5.1), available at <https://www.itu.int/md/R15-WP5A-171106-TD-0236/en>.

⁴² VLP on-body device measurements were made with two orthogonal polarized detectors and the combined total gain reported. These antennas are roughly circularly polarized, whereas traditionally FS microwave stations employ linear polarization. Thus, an average polarization loss of 3 dB is reasonable.

Mexico for every receiver, all RLANs operating within 150 km of the receiver were considered in the calculation.

Figure 5-22, Figure 5-23, and Table 5-4 show the probability of I/N (aggregated over the aforementioned morphologies) exceeding an I/N level (x-axis) due to the deployed active RLANs. Of the 2,700,000 different RLAN-FS morphologies simulated, the aggregate I/N for an FS receiver exceeded -6 dB in 0.209% of instances. Further investigation into these instances revealed that majority of them were caused by a single RLAN. Further, of these single-entry I/N > -6 dB occurrences, over half were due to an RLAN in the main beam⁴³ and 19% were due to an RLAN in the main beam of the FS receiver and less than 1 km from the FS receiver. Furthermore, there are additional topologies that resulted in a single RLAN device causing an I/N value greater than -6 dB such as: outdoor RLAN devices, indoor RLAN devices with very small building penetration loss, RLAN with minimal loss in the far-field gain (VLP), and RLAN devices having small path loss values that are statistically in the tail of the path loss probability distribution function. For all the threshold exceedance instances analyzed, none had a significant impact on FS link availability (*see section 5.2.4*).

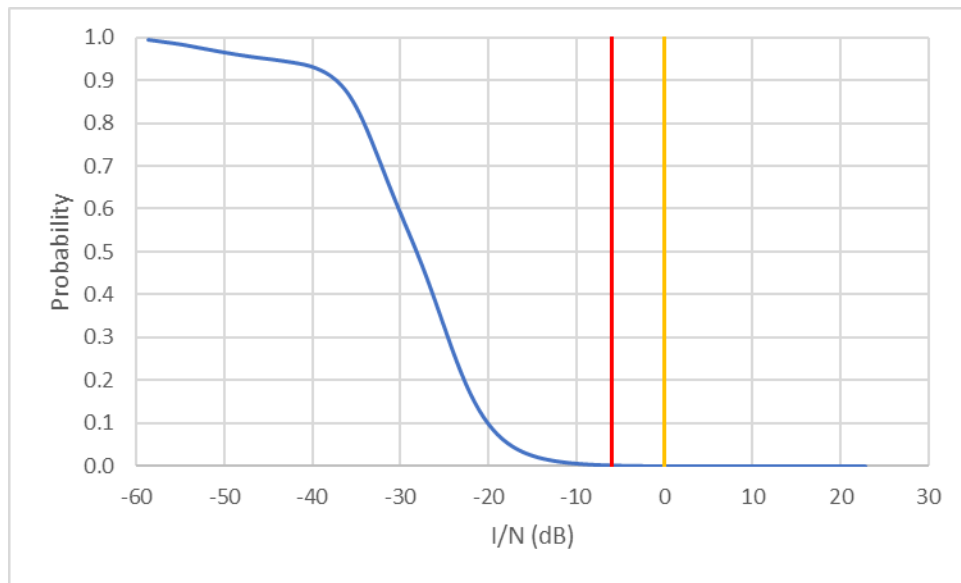


Figure 5-22 - Probability of Aggregate RLANs I/N Exceeding I/N Values on X-axis for 2,700,000 RLAN-FS morphologies (27 FS/iteration x 100,000 iterations)

⁴³ An RLAN was considered as being “in FS receiver’s main beam” if it was within FS receiver’s 3dB beamwidth, which corresponded to the RLAN being at an angle off-boresight from the FS receiver as large as 1.8° for these FS.

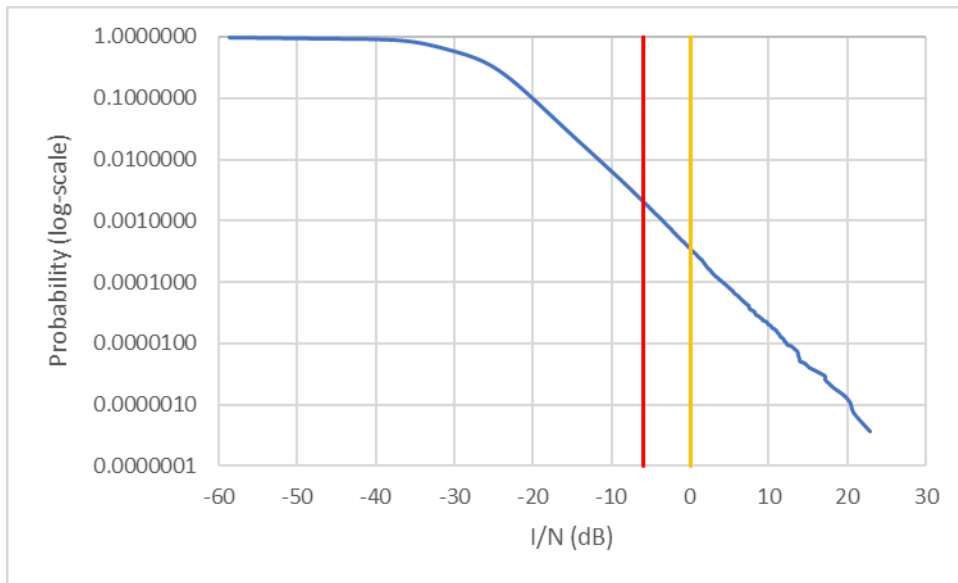


Figure 5-23 - Probability of Aggregate RLANs I/N Exceeding I/N values on X-axis for 2,700,000 RLAN-FS morphologies (27 FS/iteration x 100,000 iterations) Zoomed In

Table 5-4 - Interference statistics from 100,000 Independent Simulations of FS in Mexico City

I/N threshold (dB)	Aggregate
-6	0.209%
0	0.035%

5.2.4 FS Availability Analysis

The availability analysis assumed a typical FS design target of 99.999% availability (unavailability=0.001% corresponding to 5.3 minutes/year). Results are compared to a target increase in unavailability of less than 10%, as established by the ITU,⁴⁴ that is sufficient to allow continued robustness of FS links.

The increase in unavailability due to RLAN interference was further analyzed, using a two-step process, by looking at the 27 FS stations and at the specific impact on unavailability due to RLAN devices.

First, a fade margin required to achieve the target availability of 99.999% was determined using ITU-R Rec. P.530-17 (P.530). Then, the increase in unavailability in the presence of interference was assessed.

Second, if an FS link's unavailability increased more than 10% in Step 1, the actual operating parameters were examined to determine the available fade margin. These links were then reassessed to determine if they would meet the 10% target.

The fade margin probability density function (pdf) is obtained from P.530 (section 2.3.2 Eqn. 18) using FS unavailability and the multipath occurrence factor, p_0 . p_0 provides the fade margin required for the

⁴⁴ International Telecommunication Union, *F.1094-2: Maximum Allowable Error Performance and Availability Degradations to Digital Fixed Wireless Systems Arising from Radio Interference from Emissions and Radiations from Other Sources* (2007), available at <https://www.itu.int/rec/R-REC-F.1094/en>.

average worst month and is computed using P.530 (section 2.3.2, Eqn. 11), with input parameters from the FS data. The input parameters are the FS Transmitter (Tx) and Receiver (Rx) terrain height, antenna height above ground level, link distance, and center frequency.

Given the fade margin pdf and the pdf of the degradation due to RLAN interference for a specific FS (i.e., $(I+N)/N$ from the 100,000-iteration simulation), the impact on FS link unavailability can be determined directly from the combined distribution. The convolution provides the correct answer to this question under the assumption that the two random variables (fading and interference) are independent. This independence is a conservative approximation. In fact, there is an inverse relationship between RLAN device activity and when multipath fading occurs. As multipath fading occurs between midnight and 8 am,⁴⁵ while RLAN usage will primarily be from 7pm to 10pm (for LPI and Standard Power devices) or during daylight (for VLPs). This inverse correlation means that the sum of interference and fading is statistically smaller than what is modeled.

Furthermore, for accuracy, the full I/N distribution is used in the analysis including all aggregate interference events.

In Step 1, results showed that the 10% unavailability target was met for 8 FS (out of 27). The increase in unavailability for these 8 FS is shown in Figure 5-24. As indicated, these FS had less than 2.4% increase in unavailability.

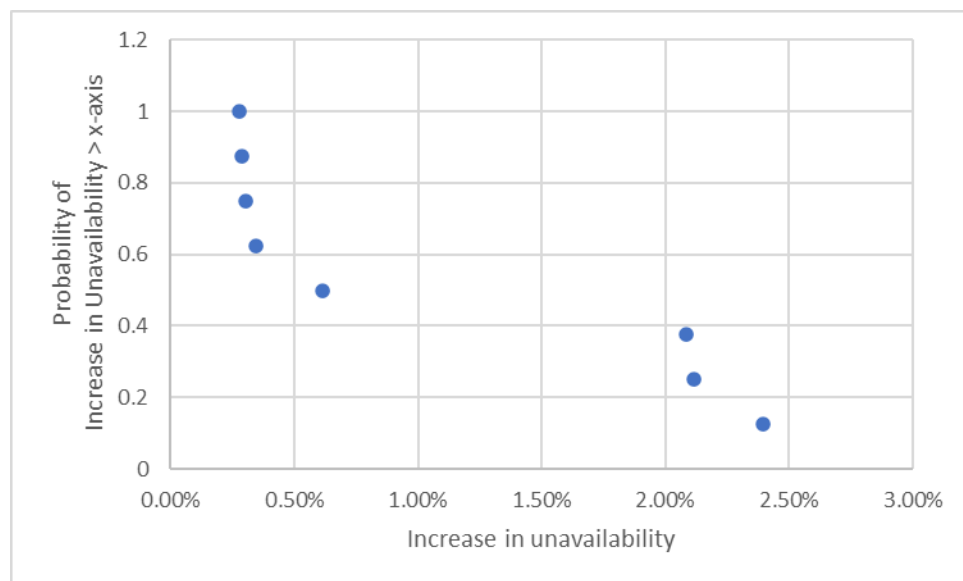


Figure 5-24 – Increase in unavailability for 8 FS that meet the 10% target.

The analysis in Step 1 assumes that each FS link has the exact margin to achieve the target availability. However, given that amplifiers and antennas only come in certain sizes, it is unlikely that these links achieve this margin exactly. In Step 2, the 19 links that failed to meet the 10% unavailability target are examined more closely. As indicated below, after considering the actual FS link operating parameters at the links' modulations in Step 2, they all meet the 10% target.

⁴⁵ See NTIA Report 05-432.

These 19 FS all had very small p_0 's (2.3×10^{-6} to 0.007) that resulted in very low fade margins (5.3 to 12.5 dB), which made them sensitive to interference. Those with $< 0.001 p_0$ are also short-haul links (≤ 15.5 Km) which have higher link margins and can generally accept interfering signals 1-10 dB or more above long-haul performance requirements and not affect long-term performance.⁴⁶

Table 5-5 shows the link characteristics of these FS stations.

Table 5-5 - Link characteristics of the FS with Increase in Unavailability > 10% using theoretical link characteristics

FS ID	FS Tx EIRP (dBm)	FS Tx Power (Watt)	FS link distance (km)	Received C/N (dB) (Eqn. 5-4)	Multipath occurrence factor, p_0 (ITU-R P.530)
2	42.16	0.00	38.39	42.71	0.002
4	42.16	0.00	38.39	42.48	0.002
6	52.494	0.03	38.39	47.97	0.002
8	62.66	0.15	38.39	63.30	0.002
9	52.494	0.03	38.39	48.05	0.002
10	42.16	0.00	38.39	42.63	0.002
12	68.4	0.72	4.49	81.99	2.26E-06
14	61.4	1.00	15.48	63.70	0.001
17	74.2	1.07	52.28	69.05	0.007
23	69.96	1.68	4.49	82.15	2.26E-06
36	42.16	0.00	38.39	42.36	0.002
38	42.16	0.00	38.39	42.13	0.003
39	51.897	0.02	38.39	46.37	0.002
40	51.897	0.02	38.39	46.22	0.002
42	62.66	0.15	38.39	62.94	0.002
44	42.16	0.00	38.39	42.28	0.003
46	68.4	0.72	4.49	81.56	2.33E-06
48	61.4	1.00	15.48	63.26	0.001
57	70.66	1.68	4.49	81.72	2.33E-06

The FS data information was used to compute the C/N at the receiver, shown in Table 5-5, using Eqn. 5-4 below:

$$\frac{C}{N} (\text{dB}) = \text{EIRP} (\text{dBW}) - \text{FSPL} (\text{dB}) - L_{feed} (\text{dB}) + G_R (\text{dBi}) - N (\text{dBW}) \quad (5-4)$$

where,

- EIPP (dBW) = FS EIRP from the FS data

⁴⁶ National Telecommunications and Information Administration, *Interference Protection Criteria Phase 1 - Compilation from Existing Sources*, NTIA Report 05-432, 4-8, 4-9 (2005), https://www.ntia.doc.gov/files/ntia/publications/ipc_phase_1_report.pdf (“NTIA Report 05-432”).

- FSPL (dB) = $92.45 + 20\log_{10}(\text{FS link distance [km]}) + 20\log_{10}(\text{center frequency [GHz]})$
- L_{feed} = FS Rx Feederloss from the FS data
- G_R = FS Rx Gain (dBi) from the FS data
- N = Noise Power (dBW) = $-228.6 \text{ dB}(W/K/Hz) + 10\log_{10}(T) + \text{Noise Figure} + 10\log_{10}(B [\text{Hz}])$
- T = System temperature = 290 K
- Noise Figure = 4 dB from the FS data
- B = FS channel bandwidth (Hz)

The actual FS fade margin, F_a , is then computed as shown in Eqn. (5-5).

$$F_a (\text{dB}) = C/N (\text{dB}) - (\max) C/N_{\text{req}} (\text{dB}) \quad (5-5)$$

The modulations in the FS data for the 19 FS links were: Analog Modulation, 64QAM, 128QAM or 256QAM.

Table 5-6 shows C/Nreq values obtained from several manufacturers' datasheets. The 30 MHz channels have a range of values that indicate different coding and receiver performance. For the analysis, the maximum C/Nreq values are used (indicated in **bold**). This will provide the most conservative answer.

Note that the 19 FS have the following bandwidths for each modulation. For the FS bandwidths unavailable in manufacturers' datasheets, the closest lower bandwidth is chosen as indicated below for conservativeness.

- Analog Modulation: 11.8 and 24.3 MHz → 10 and 20 MHz
- 64-QAM: 7 and 24.3 MHz → 7 MHz
- 128-QAM: 35 MHz → 30 MHz
- 256-QAM: 25.8 MHz → 20 MHz

Furthermore, for Analog Modulation, the C/Nreq for 64-QAM modulation was chosen for conservativeness.

Table 5-6 - SNR required used for the 19 FS based on the link's modulation and bandwidth

Modulation	Bandwidth (MHz)	C/Nreq (dB)	Manufacturers
64-QAM	30	16.7 – 20.7	SAF Integra, Redline RDL 5000, and ALFOplus ⁴⁷
128-QAM		19.7 – 24.2	
64-QAM	7	22.5	SAF Integra

⁴⁷ See SAF Tehnika, *SAF Integra Datasheet*, <https://www.ispsupplies.com/content/datasheets/Integra%20series%20DS%20v1.43.pdf>; Redline Communications, *RDL-5000 Datasheet*, <https://rdlcom.com/wp-content/uploads/Redline-DS-RDL-5000.pdf>; SIAE Microelettronica, *ALFOplus2 Datasheet*, available at <https://www.siaemic.com/index.php/products-services/telecommunication-systems/microwave-product-portfolio/alfoplus2>.

64-QAM	10	20.5	SAF Integra
64-QAM	20	17.0	Redline RDL 5000
256-QAM	20	23.5 (strongFEC ⁴⁸⁾ 27.0 (weakFEC)	Redline RDL 5000

Table 5-7 summarizes the key performance parameters for each link including the Fade Margin (FM) at the 99.999% availability target, the received C/N (Eqn. 5-4), C/Nreq (from Table 5-11), and F_a (Eqn. 5-5). The actual link fade margin is then compared to the FM at 99.999% availability and the difference is the “Actual Margin Above FM” (column C5). Notice the calculated “Actual Margin above FM” is very high for these links (>10.95 dB).

In addition, Table 5-7 includes the three FS (see Figure 5-24) that met 10% increase in unavailability but not 1% in the last 3 rows.

Next, the additional margin to meet the 10% target is determined and is shown in column C6.

Finally, the “Actual Margin above FM” (C5) is compared against the “Increase in FS link margin to meet the 10% target” (C6). The results show that the actual operating parameters on these 19 links led to more than sufficient margin to meet the 10% target.

To further demonstrate the robustness of this analysis, 1% increase in unavailability was studied as a sensitivity analysis and shown in column C7. As indicated in (C6) and (C7), the overall interference risk from RLAN operations is so low that nearly the same margin is necessary to achieve both 10% and 1% increase in unavailability.

This shows that all the 27 FS links meet the 10% increase in unavailability target as well as the sensitivity analysis down to 1% increase in unavailability.

Table 5-7 - FS with Increase in Unavailability > 1% had “Actual Margin beyond FM” (C5) >> “Increase in FS Link Margin to meet 10% target (C6) and 1% sensitivity (C7)”

FS ID	FM (dB) @ 99.999%	Received C/N (dB) (Eqn. 5-4)	C/Nreq (dB)	F _a (dB) (Eqn. 5-5)	Actual Margin (dB) above FM	Increase in FS Link Margin (dB), x, to meet 10% target	Increase in FS Link Margin (dB), x, to meet 1% (sensitivity)
Column	C1	C2	C3	C4=C2- C3	C5=C4- C1	C6	C7
2	10.57	42.71	20.5	22.21	11.65	0.70	0.79
4	10.60	42.48	20.5	21.98	11.38	4.05	4.05
6	10.50	47.97	17	30.97	20.47	0.55	0.65
8	10.56	63.30	20.5	42.80	32.25	0.14	0.26
9	10.49	48.05	17	31.05	20.56	2.04	2.04
10	10.58	42.63	20.5	22.13	11.55	0.42	0.53
12	5.32	81.99	27	54.99	49.67	11.96	12.86
14	8.70	63.70	22.5	41.20	32.50	4.95	4.95
17	12.34	69.05	24.2	44.85	32.52	4.85	4.85
23	5.32	82.15	27	55.15	49.83	9.28	9.92
36	10.65	42.36	20.5	21.86	11.21	5.20	5.20

⁴⁸ FEC = Forward Error Correction Coding

38	10.68	42.13	20.5	21.63	10.95	5.42	7.03
39	10.56	46.37	17	29.37	18.80	2.76	2.76
40	10.58	46.22	17	29.22	18.63	0.44	0.54
42	10.64	62.94	20.5	42.44	31.80	5.77	10.15
44	10.66	42.28	20.5	21.78	11.12	5.93	6.51
46	5.33	81.56	27	54.56	49.23	13.80	14.10
48	8.74	63.26	22.5	40.76	32.02	7.50	10.07
57	5.33	81.72	27	54.72	49.39	3.61	3.65
13	12.36	69.25	24.2	45.05	32.69	N/A ⁴⁹	0.03
18	12.36	71.41	24.2	47.21	34.84	N/A	0.03
22	12.35	71.21	24.2	47.01	34.67	N/A	0.02

5.2.5 FS Sharing Conclusions

To assess the interference impact from RLAN devices to FS stations, 100,000 Monte-Carlo simulation iterations were run for 27 FS in the vicinity of Mexico.

The simulation results indicated low average I/N > -6 dB and 0 dB occurrence probabilities of 0.209% and 0.035% respectively.

To accurately assess the impact of RLAN interference on FS performance, the increase in FS unavailability was computed for all 27 FS. The increase in FS unavailability analysis showed that using ITU derived fading distributions and considering the operating parameters of the FS, the increase in unavailability did not exceed the 10% target and the 1% sensitivity threshold for all 27 FS.

In conclusion, RLANs in the three device classes operating over a 20, 40, 80, or 160 MHz channel bandwidth do not cause harmful interference to an FS uplink.

5.3 MSS Gateway Coexistence

This Section describes analyses performed to examine the risk of harmful interference to the earth station antenna at the sole MSS gateway site, under construction, for each of the three RLAN device classes and the total number of RLAN devices. The analysis specifically addresses item number 14 in Table 2 of the IFT reference document - MOBILE SATELLITE SERVICES MÉXICO, S. DE R.L. DE C.V. Mobile Satellite Services Mexico is authorized to operate a constellation of non-geostationary low earth orbit ('LEO') satellites of the MSS, which use the frequency segment 6875-7075 MHz for its downlink links from the satellite constellation to roughly two dozen FSS receive sites (referred to in this document as MSS gateways) around the world.

There are two MSS satellite constellations on file with the ITU. They are HIBLEO-4FL and HIBLEO-X. Each constellation consists of 24 satellites with 3 satellites per orbital plane and 8 orbital planes. HIBLEO-4FL is the older of the two constellations. The downlink from the satellite to the MSS gateway site operates on 6875-6877.25 MHz. The space-to-earth downlink in the replacement constellation, HIBLEO-X, can operate between 6875-7075 MHz. Due to its much larger nominal frequency range, the simulation uses only the 24 satellites in the HIBLEO-X satellite network.

⁴⁹ 10% availability was met for this FS.

5.3.1 MSS Gateway Characteristics

The geo-coordinates the MSS gateway earth station was provided by IFT from licensing information on file. Once completed, the site will be the only MSS gateway in Mexico. The site is located in an isolated valley north and west of Mexico City in Jocotitlán, State of Mexico. A terrain map taken from Google Maps is presented below.

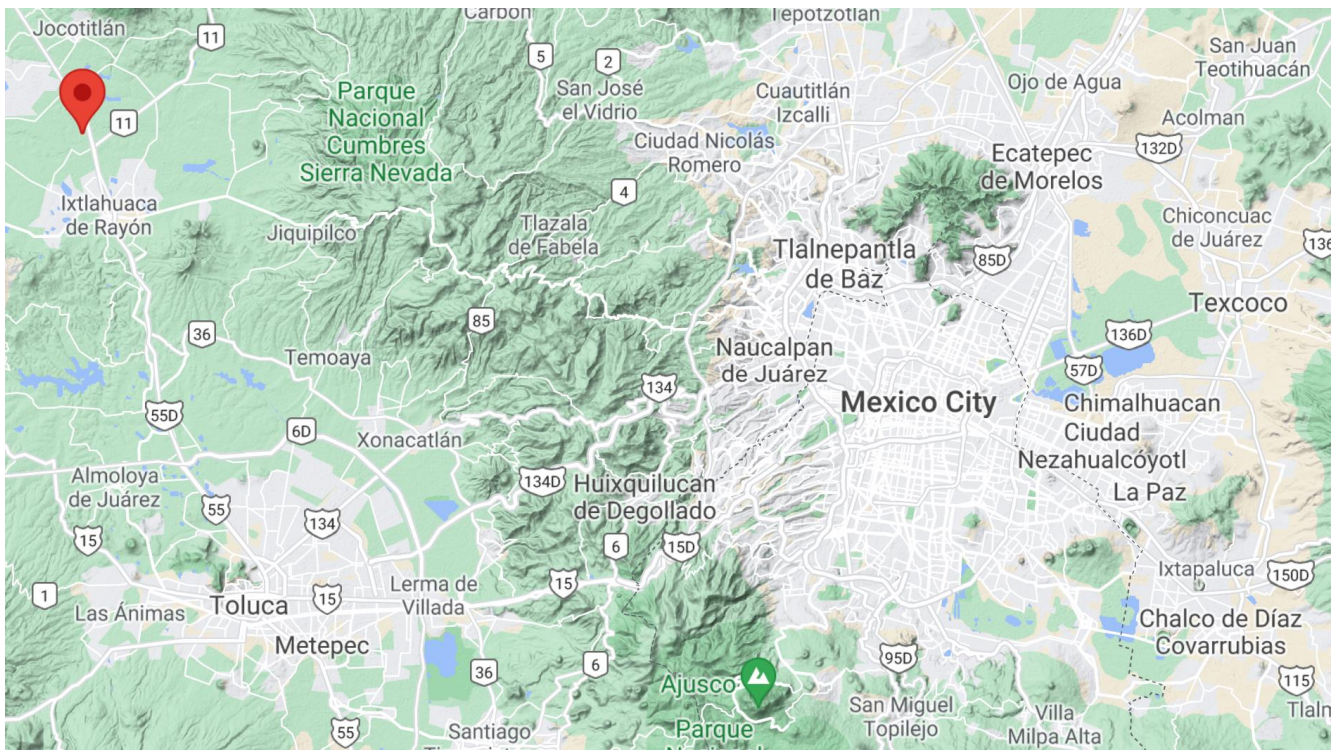


Figure 5-25 – Terrain Map of MOBILE SATELLITE SERVICES MÉXICO, S. DE R.L. DE C.V Gateway Site Within Central Mexico

A closer look at the immediate area around the MSS gateway site using Google Maps shows there is limited development. Presumably, this was one of the reasons for the site being selected for the new MSS gateway.

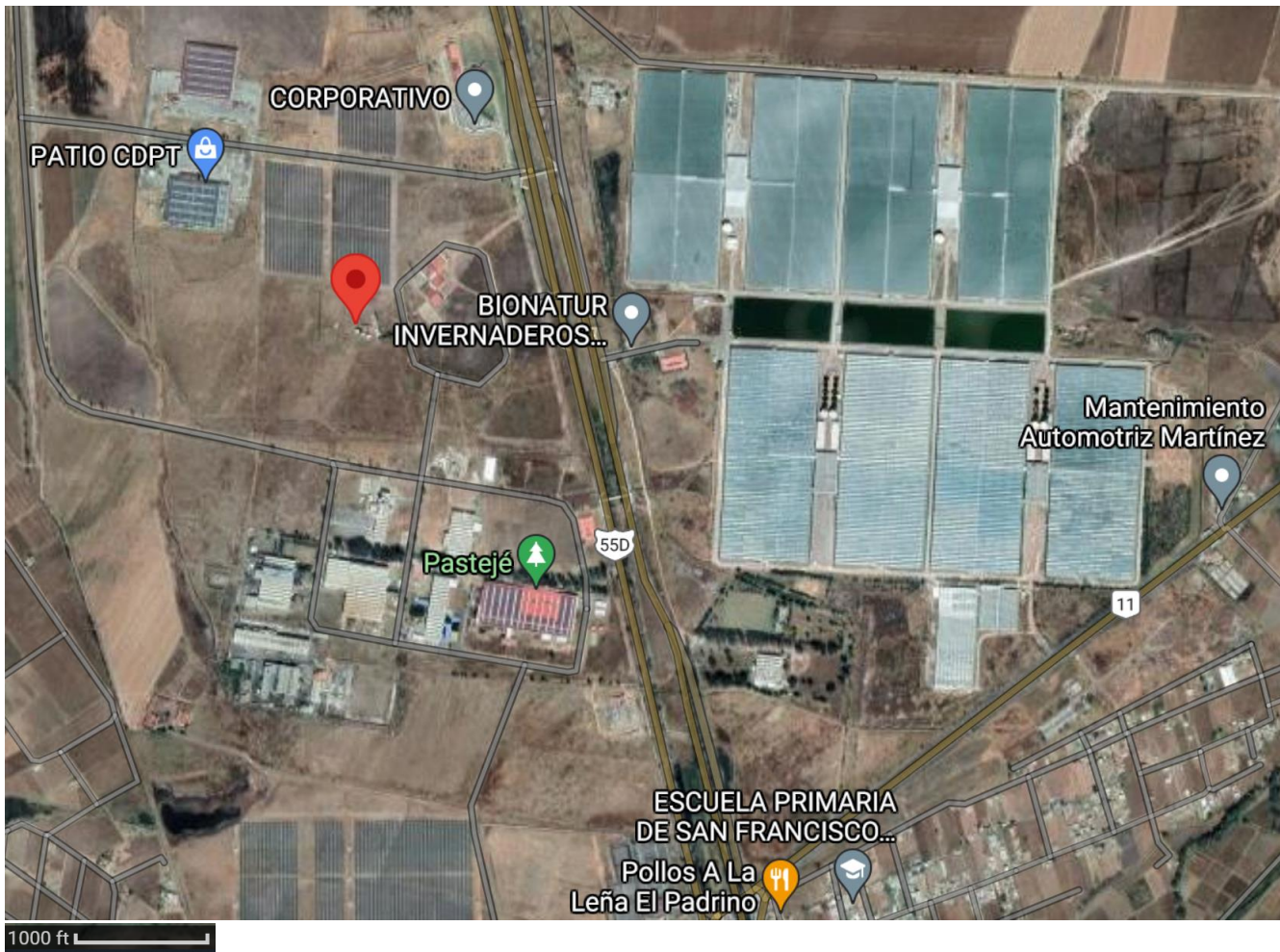


Figure 5-26 – Local Area Surrounding MSS Gateway Site (earth station antenna location noted in red)

A close up of the MSS gateway site shows that once completed there will be four earth station antennas. Based on earth station antenna deployments at MSS gateways in the United States and Canada, only the uppermost antenna appears to be in its final location. For this reason, the simulations use the coordinates and characteristics of uppermost antenna.



Figure 5-27 – MSS Gateway Site Under Construction

The MSS gateway characteristics used for the Monte Carlo simulation are provided below.

Table 5-8 – MSS Gateway Characteristics

Parameter	Value	Comments
Number of Antennas	1	
Latitude	19.63266, -99.785807	
Longitude		
Antenna Pattern	ITU-R S.465-6	Per License
Antenna Diameter	5.5 meters	Per license
Gain	50.2 dBi	
System Noise Temp (T in KTB) (includes feederloss)	186.2087 K = $10^{((50.2 - 27.5) (G/T))/10}$ Noise Figure = -1.92398 dB	
Frequency Channel	6875 – 7055 MHz (180 MHz bandwidth)	One CDMA carrier (per license)
Elevation angle	Randomly chosen from a generated distribution	TBD
Polarization	Circular	
AGL Height	4 meters	

5.3.2 RLAN Device Characteristics

As the analysis examines the potential risk of harmful interference from each class of RLAN device, the number of units in each class must be determined. For the Monte Carlo studies on FSS and FS in the previous sections, the aggregate number of indoor and outdoor RLAN units were considered. The only difference in the assumptions from the previous studies is that in this instance, the number of

RLAN units are separated by RLAN class in order to derive the percentage (and number) of RLAN units for each.

Table 5-9 – Percentage of RLAN Units by Regulatory Class

RLAN Class	Units (percent)		
	Indoors	Outdoors	Total
LPI and LPI Clients	79.56	-----	79.56
Standard Power and Clients	8.44	1	9.44
VLP	10	1	11
Total	98	2	100

Note that the sum of the number of LPI and Standard Power units remains 88 percent, which is same as before. In addition, separate EIRP distributions for LPI and indoor standard power devices were generated. A table of the revised weighted EIRP distributions for LPI and Standard Power devices used in the simulations are presented below.

Table 5-10 – Revised LPI and Indoor Standard Power EIRP Distribution

Revised - LPI		Weighted EIRP Distribution (mW)							
Indoor Use Case	Weight	4000	1000	250	100	50	13	1	Total
Client (LPI)	24.10%	0%	0%	0%	1.08%	10.68%	12.34%	0%	24.10%
Consumer AP (LPI)	66.31%	0%	0%	7.90%	2.76%	11.20%	38.94%	5.51%	66.31%
Sub-Total	90.41%	0.00%	0.00%	7.90%	3.84%	21.88%	51.28%	5.51%	90.41%
Distribution		0.00%	0.00%	8.74%	4.24%	24.21%	56.72%	6.09%	100.00%
Revised - Indoor SP		Weighted EIRP Distribution (mW)							
Indoor Use Case	Weight	4000	1000	250	100	50	13	1	Total
Client (SP)	2.22%	0%	0%	0%	0.74%	1.35%	0.13%	0%	2.22%
Enterprise AP (SP)	2.63%	0%	0%	1.06%	0.90%	0.58%	0.08%	0.01%	2.63%
High-Performance									
Gaming Router (SP)	4.74%	0.67%	0.42%	1.43%	1.01%	0.83%	0.34%	0.04%	4.74%
Sub-Total	9.59%	0.67%	0.42%	2.49%	2.65%	2.76%	0.55%	0.05%	9.59%
Distribution		6.98%	4.38%	25.96%	27.67%	28.72%	5.77%	0.52%	100.00%

5.3.3 MSS Simulation Methodology

A Monte-Carlo simulation with 100,000 iterations was run to characterize the interference from the three classes of RLANs (LPI, VLP and Standard Power) to the earth station antenna at MSS gateway location. The RLANs were dropped per the methodologies and operating assumptions described in Section 5.2 for sharing with the FS links. This resulted in a total of 4.8 billion (or 4,803,200,000) RLAN drops within 150 km of the earth station antenna at the MSS gateway over the 100,000 iterations (48,032 drops per iteration). The weighted EIRP distribution were used from Table 5-10.

The distributions of pointing directions for the MSS gateway earth station antenna are generated using a separate simulation of the MSS constellation per MSS Gateway characteristics (Table 5.8) and system parameters in the table below.

Table 5-11 – MSS Constellation System Parameters

MSS Constellation Parameter	Value
Number of LEO Satellites	24 (3 satellites /plane x 8 orbital planes)
Orbital Plane Inclination	52°
Satellite Altitude	1,409.78 km

The figure below, a screen shot taken from the IFT's Map of Non-Geostationary Satellites with Footprint in Mexico for the sole MSS satellite constellation with a downlink between 6875-7075 MHz, provides a snapshot of the satellites in view of the MSS gateway at a random moment in time. Over time, various satellites in the constellation will pass within view over the MSS gateway at different elevation angles. The screen shot is meant to be illustrative of the MSS constellation modeling and overall methodological approach.

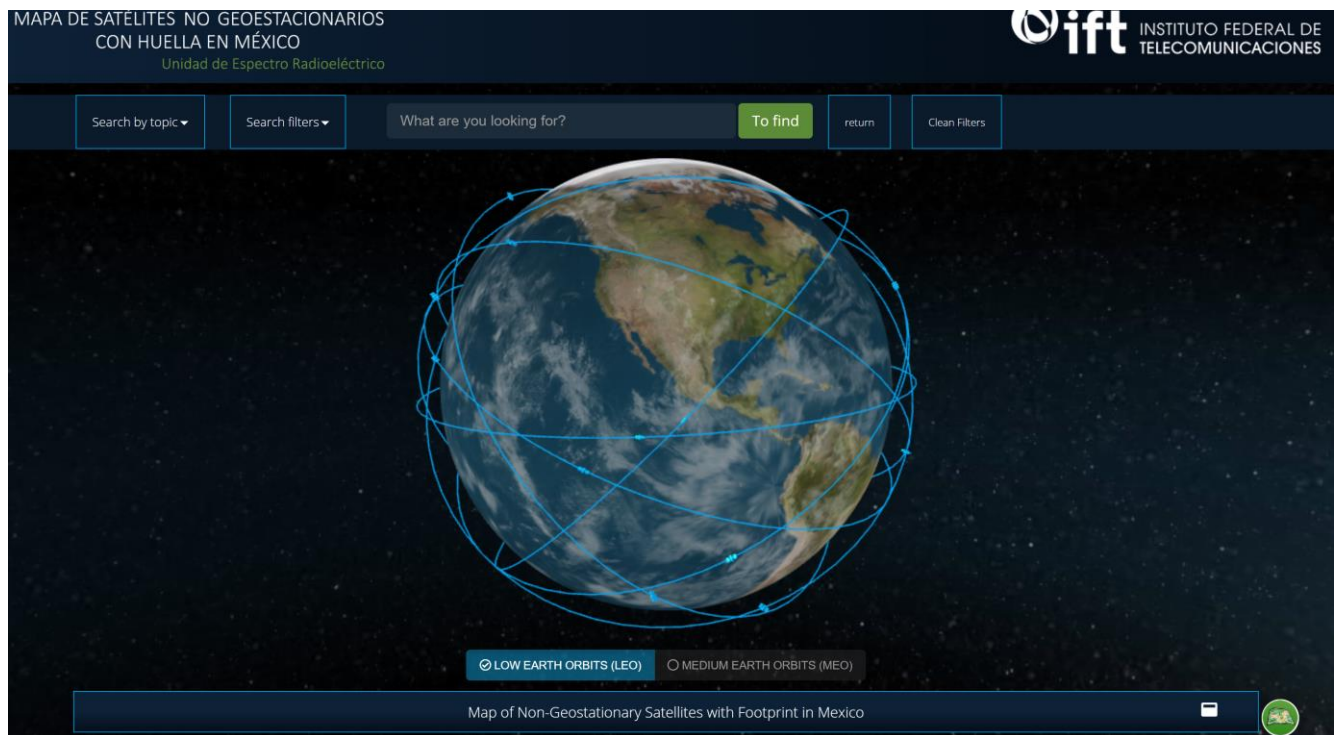


Figure 5-28 – Screenshot of IFT Map of Non-Geostationary Satellites with Footprint in Mexico with a 6875-7075 MHz Downlink⁵⁰

The movement of the MSS constellation is plotted over time as viewed from the MSS gateway earth station antenna. In each of the 20,000 iterations, the pointing direction of the earth station antenna is chosen randomly from one of the 50,000 that is generated by simulating the MSS constellation's movement. At each snapshot in time, the earth station antenna pointing direction is chosen by picking randomly, one of the satellites that is above the radio horizon. The minimum elevation angle is assumed to be 10 degrees.

The CDF of the earth station antenna elevation is plotted below. Note that about two-thirds of the earth station elevation angles are below 30 degrees, 90 percent of the satellites are below 50 degrees, and there are no earth station elevation angles above 80 degrees (no satellites directly overhead).

⁵⁰ <http://mapasatelital.ift.org.mx/nogeostacionarios#>

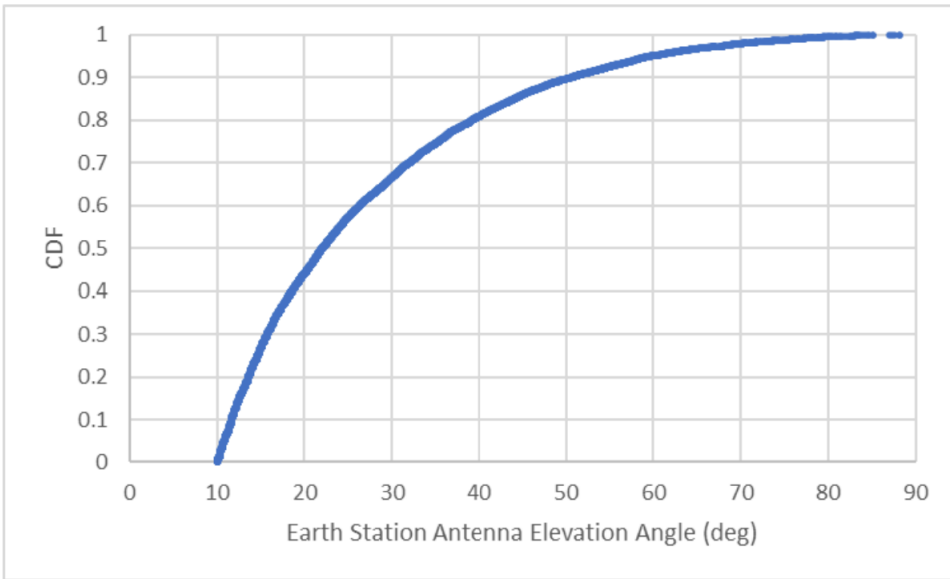


Figure 5-29 – CDF of Earth Station Antenna Elevation Angles

5.3.4 MSS Simulation Results

The cumulative probabilities of I/N were calculated for each of the three RLAN classes and for the total number of RLAN devices and are presented in Figure 5-30 below.

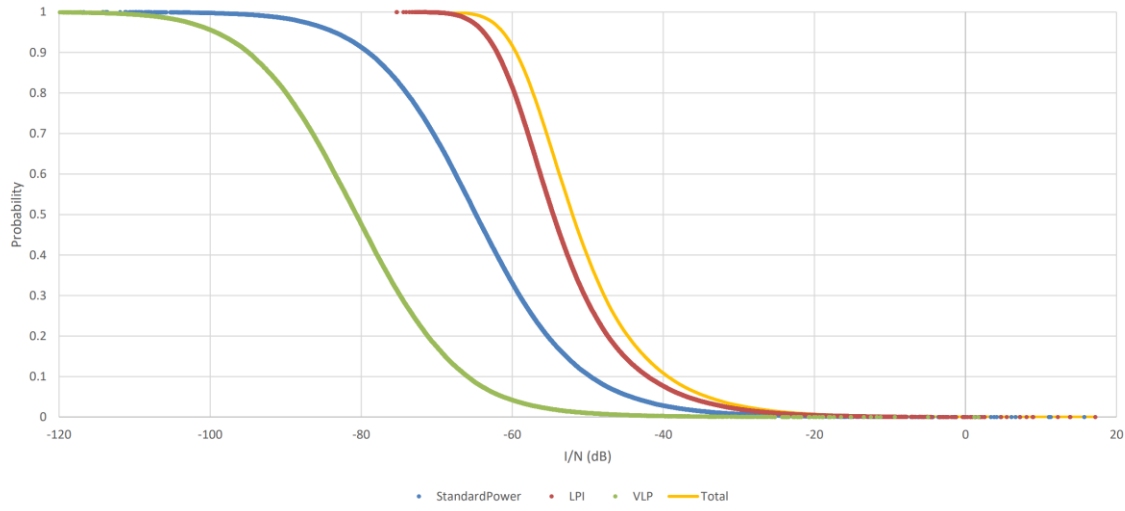


Figure 5-30 – Cumulative Probabilities of I/N by RLAN Class and Total RLANs

Table 5-13 shows the cumulative probability of I/N exceeding values of -6 dB and -12.2 dB. Of the three RLAN classes, LPI devices have the highest I/N at a given probability because LPI devices make up nearly 80 percent of all RLAN units.

Table 5-12 – Cumulative Probabilities of I/N Exceeding -6 dB and -12.2 dB for Each RLAN Class and Total RLANs

I/N	Standard Power	LPI	VLP	Total
-6 dB	0.031%	0.049%	0.003%	0.083%
-12.2 dB	0.070%	0.146%	0.006%	0.223%

The probability of each RLAN class exceeding and I/N of -6 dB and and I/N of -12.2 dB is exceedingly small. This becomes even more evident when the ‘tail’ of I/N values in figure xx is expanded. For comparison purposes, in Table 5-5, the cumulative probability of RLANs exceeding -6 dB with respect to FS links is 0.209%.

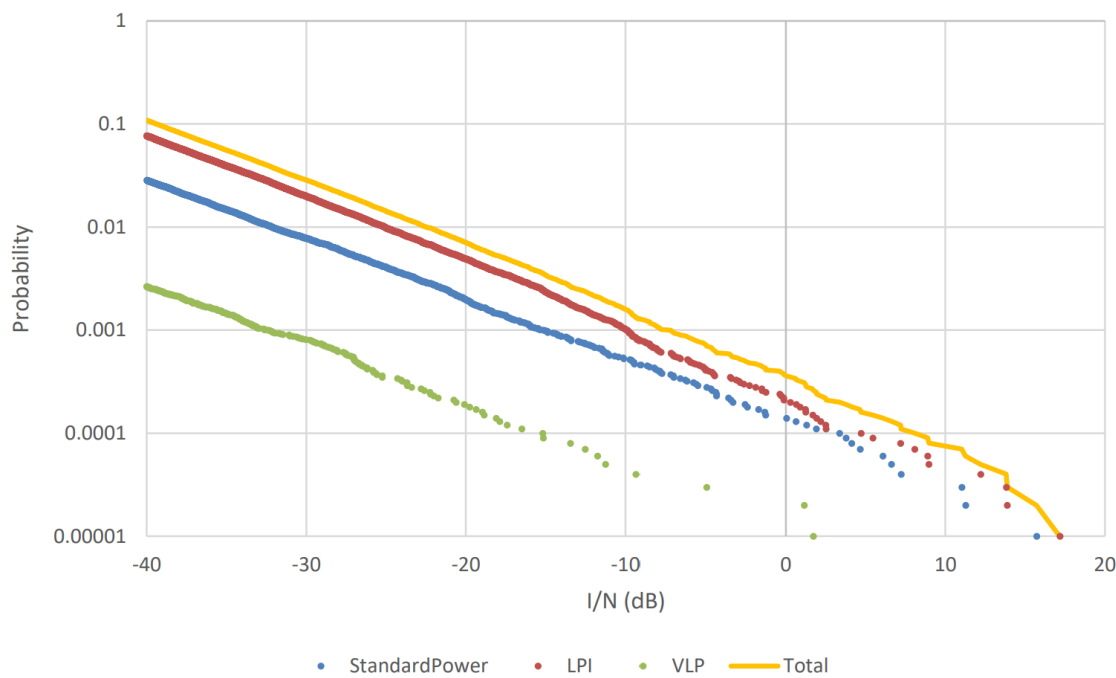


Figure 5-31 – Cumulative Probability I/N Greater Than -40 dB by RLAN Class and Total RLANs

The Monte Carlo study did not consider any mitigations. For example, if IFT were to allow Standard Power RLANs across the entire 6 GHz band under the condition that an Automated Frequency Coordination is required, co-channel operation would be prevented in proximity of the MSS gateway site. The MSS operator could create physical barriers (e.g., plant trees, build a berm) and work with its neighbors around the MSS gateway site to further reduce the already minimal probability of an exceedance of the IPC.

5.3.5 MSS Gateway Coexistence Sharing Conclusions

The cumulative probabilities of I/N are presented for Standard Power, LPI, and VLP RLANs separately, considering MSS constellation and MSS gateway earth station coordinates and characteristics, assumptions regarding the characteristics and deployments of each RLAN class, and for random earth station pointing angles. The results of these studies clearly show that the risk of harmful interference to the future MSS gateway site’s earth station antenna from Standard Power, LPI, and VLP RLAN devices is extremely low.

This result is consistent with the conclusion reached by the US FCC reached with respect to the domestic MSS gateway sites operated by Globalstar, Inc.

In its 6 GHz Report and Order the US FCC said, “Globalstar which operates earth stations receiving in the U-NII-8 band, claims that allowing indoor use of the U-NII-8 band would cause substantial harmful interference to its existing MSS feeder downlinks, and to any additional gateways that it may consider deploying in the future...With regard to earth station receivers, we disagree with Globalstar’s analysis...[we] find that Globalstar’s link budget analysis fails to fully consider all the probability factors that must align in order for interference to occur. We therefore find that the risk of harmful interference occurring to Globalstar’s earth stations to be low.”⁵¹

In conclusion, RLAN’s in the three device classes -- Standard Power, LPI, and VLP -- do not cause harmful interference to the earth station antenna at the MSS gateway site.

⁵¹ See 6 GHz Report & Order at ¶¶ 170-172.